Vietnam Journal of Earth Sciences, 47(1), 104-132, https://doi.org/10.15625/2615-9783/21915

Vietnam Journal of Earth Sciences
https://vjs.ac.vn/index.php/jse

Some characteristics of sediments in Cenozoic basins in Northern Vietnam: implication for Oligocene paleoclimate

Mai Thanh Tan[1*], Dinh Van Thuan[1], Le Duc Luong[1], Tran Thi Thuy Van[2], Ngo Thi Dao[1]

[1]*Institute of Geological Sciences, Vietnam Academy of Science and Technology, Hanoi, Vietnam*
[2]*Institute of Geography, Vietnam Academy of Science and Technology, Hanoi, Vietnam*

Received 12 July 2023; Received in revised form 30 September 2023; Accepted 08 November 2024

ABSTRACT

Oligocene sediments in northern Vietnam have been extensively studied in terms of geology, stratigraphy, paleogeography, formation environments, tectonics, etc. However, relatively little attention has been paid to the paleoclimate. The Oligocene climate interpreted herein is based on features recorded in sediments taken from the Dong Ho (Hoanh Bo basin), Na Duong (Na Duong basin), and Co Phuc (Red River Trough) formations. These sediments were analyzed using thin-section microscopy, X-ray diffraction, and palynology with the Coexistence Approach. The sediments primarily consist of conglomerate, gritstone, sandstone, siltstone, claystone, and coal shale, deposited in continental environments and dated to the Oligocene based on palynomorph assemblages. The Oligocene paleoclimate is generally warm subtropical, with intermittent hot-humid or cold-dry periods and a slight influence of monsoons. An alternation of hot-humid and cold-dry climates was recorded in the Hoanh Bo basin. In the Red River Trough, the Oligocene climate exhibited a Mean Annual Temperature (MAT) of 9.3-22.2°C and a Mean Annual Precipitation (MAP) of 1122 to 1857 mm, based on the majority of palynological samples, indicating more continental, drier and colder conditions than present. In the Na Duong basin, a warm subtropical climate with a MAT of 9.3-21.7°C and MAP of 1122-1724 mm in the majority of samples was occasionally replaced by hot and humid subtropical periods; the variations in temperature and precipitation followed a similar pattern, suggesting an alternation between dry-cold and humid-hot phases.

Keywords: Oligocene, paleoclimate, northern Vietnam, palynomorphs, Coexistence Approach, thin section, X-ray diffraction.

1. Introduction

Cenozoic sediments, particularly those from the Oligocene epoch in northern Vietnam, have received considerable attention primarily for prospecting and exploring mineral resources, especially energy. Extensive studies have been conducted on their geological characteristics and paleogeographic and environmental interpretations, utilizing methods such as seismic stratigraphy, sequence stratigraphy, seismic wave analysis, well logging, sedimentary lithology and petrology, clay mineral analysis, and paleontological assessments, including pollen and spores, foraminifera, etc. However, there have been relatively few studies focusing on paleoclimate, as interpreted from palynological analyses (Duong and Linh,

*Corresponding author, Email: maithanhtan@igsvn.vast.vn

2011; Thuan et al., 2019; Wysocka et al., 2022; Huang et al., 2022), paleontological analysis (Böhme et al., 2010), as well as petrological, mineralogical and geochemical analyses (Long et al., 2010, Tha et al., 2017, 2021; Vuong and Hoai, 2018; Wysocka et al., 2022, Quang et al., 2023) and magnetic susceptibility (Huong et al., 2022; Lan et al, 2023). Quantitative paleoclimate assessments have also been mentioned, focusing on mean annual precipitation (MAP) based on the integration of geochemical data and chemical weathering indexes (Vuong and Hoai, 2018), and mean annual temperature (MAT) and MAP derived from palynological data using the Coexistence Approach (CA) (Thuan et al., 2019). The present study aims to highlight significant features of Oligocene sediments that allow for paleoclimate interpretation in both qualitative and quantitative terms. This research contributes new insights into Oligocene paleoclimatology in Vietnam and provides localized details regarding the general paleoclimate during this epoch worldwide.

2. Geological setting

The Cenozoic basins in northern Vietnam were formed as a result of the collision between the Indian and Eurasian plates, large-scale left strike-slip movement along the Red River fault zone accompanied by the clockwise rotation of the Indochina block (Tapponnier et al., 1986) and the opening the East Sea (Lee and Lawver 1995; Chung et al., 1997). The Red River fault zone exhibited a sinistral offset of approximately 330±60 km during the Paleogene to Neogene (Lacassin et al., 1993), with estimates ranging from 500 to 700 km (Leloup et al., 1995). However, during the Pliocene to Quaternary, movement along this fault zone shifted to dextral, with offsets ranging from 0.15 to 2.5 km and rates of 0.3 to 0.56 mm/year (Trinh et al., 2012), or an amplitude of 0.4 to 5.3 km, equivalent to 0.43-1.1 mm/year (Zuchiewicz et al., 2013). The sedimentary evolution in northern Vietnam, related to Cenozoic geodynamic activities, is prominently expressed in the Red River Basin, which comprises seven sedimentary cycles of Eocene, Oligocene, Lower Miocene, Middle Miocene, Upper Miocene, Pliocene, and Quaternary (Nghi et al., 2004). Paleogene to Miocene sediments in northern Vietnam are found in the Hoanh Bo, Na Duong, That Khe, and Cao Bang basins in the northeastern region, the Red River trough and Ha Noi depression in the central area, and the Muong Te and Song Da basins in the northwestern region. These sediments were primarily deposited in fluvial, lacustrine and deltaic environments, distributed within intramountain depressions and pull-apart grabens controlled by major NW-SE faults, such as Cao Bang - Lang Son, Song Lo, Vinh Ninh, Song Chay, Song Hong (Thanh et al., 2005).

The field survey and sampling in this study focus on the Oligocene sediments in the Hoanh Bo and Na Duong basins and the Red River Trough (Figs. 1, 2). The Hoang Bo basin contains two Tertiary formations: the Dong Ho Formation, which is 150 meters thick and consists of siltstone, oil shale, sandstone and claystone intercalated with conglomerate and thin layers of coal shale; and the Tieu Giao Formation, which ranges from 20 to 200 meters in thickness and is composed of sandstone, siltstone and claystone (Luong et al., 1999; Ky et al., 1999) (Fig. 3). The Na Duong basin is filled with fluvial and lacustrine deposits, including the Na Duong Formation, which is 295 meters thick and comprises coaly shale, siltstone, sandstone, as well as seams and lenses of lignite; and the Rinh Chua Formation, which is 270 meters thick and consists of claystone, siltstone, and brown medium- to coarse-grained sandstone (Ky et al., 2000). The Red River Trough contains two Oligocene formations: the Van Yen Formation, composed of conglomerate with lenses of sandstone; and the Co Phuc Formation, which

includes conglomerate, gravelstone, clay shale, coal shale, and coal lenses, ranging from in 1,000 to 1,300 meters in thickness (Vinh et al., 2005).

This study focused on the Dong Ho formation in the Hoanh Bo basin, the Na Duong formation in the Na Duong basin, and the Co Phuc formation in the Red River Trough. Previous studies have mentioned these formations petrologically, including Huyen et al. (2004), Wysocka & Swierczewska (2010), Long et al. (2009), Tha et al. (2015, 2017), and Wysocka et al. (2020, 2022).

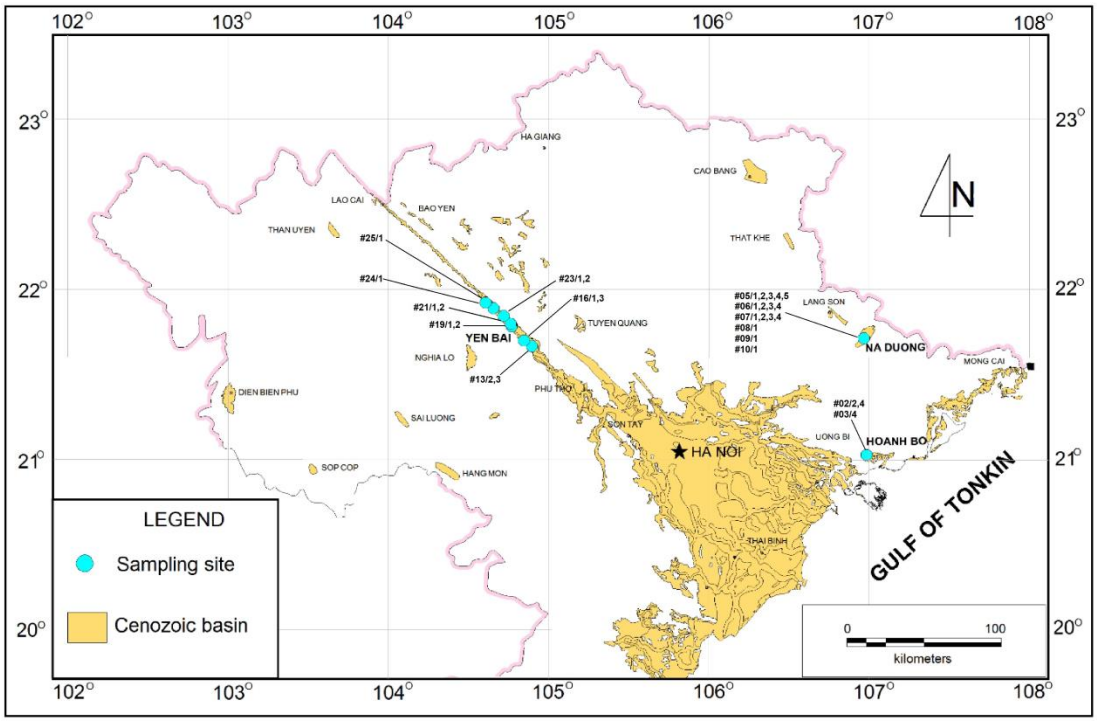

Figure 1. Cenozoic basins in North Vietnam and sampling sites

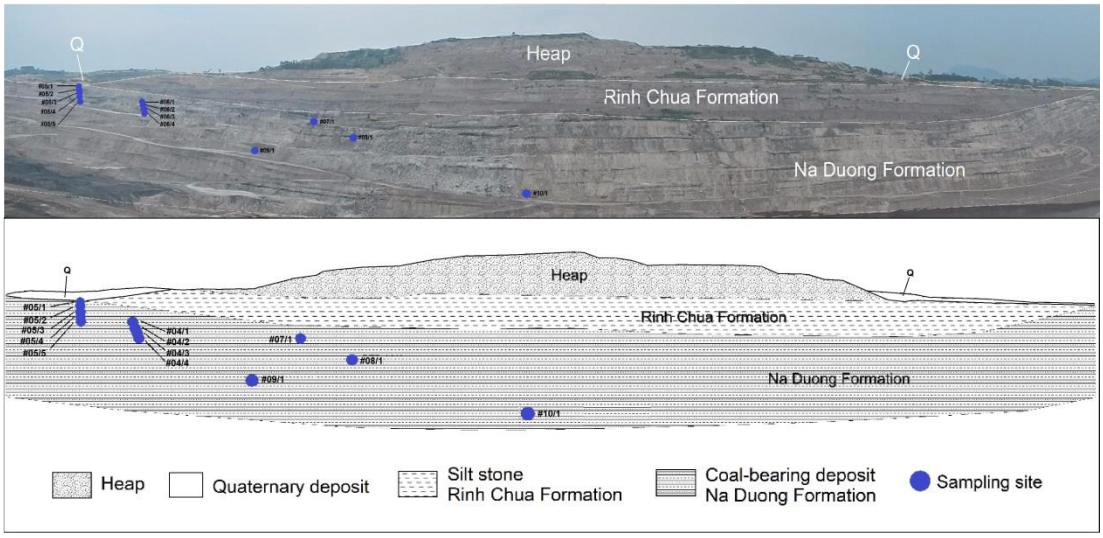

Figure 2. Cross-section in Na Duong basin with sampling sites

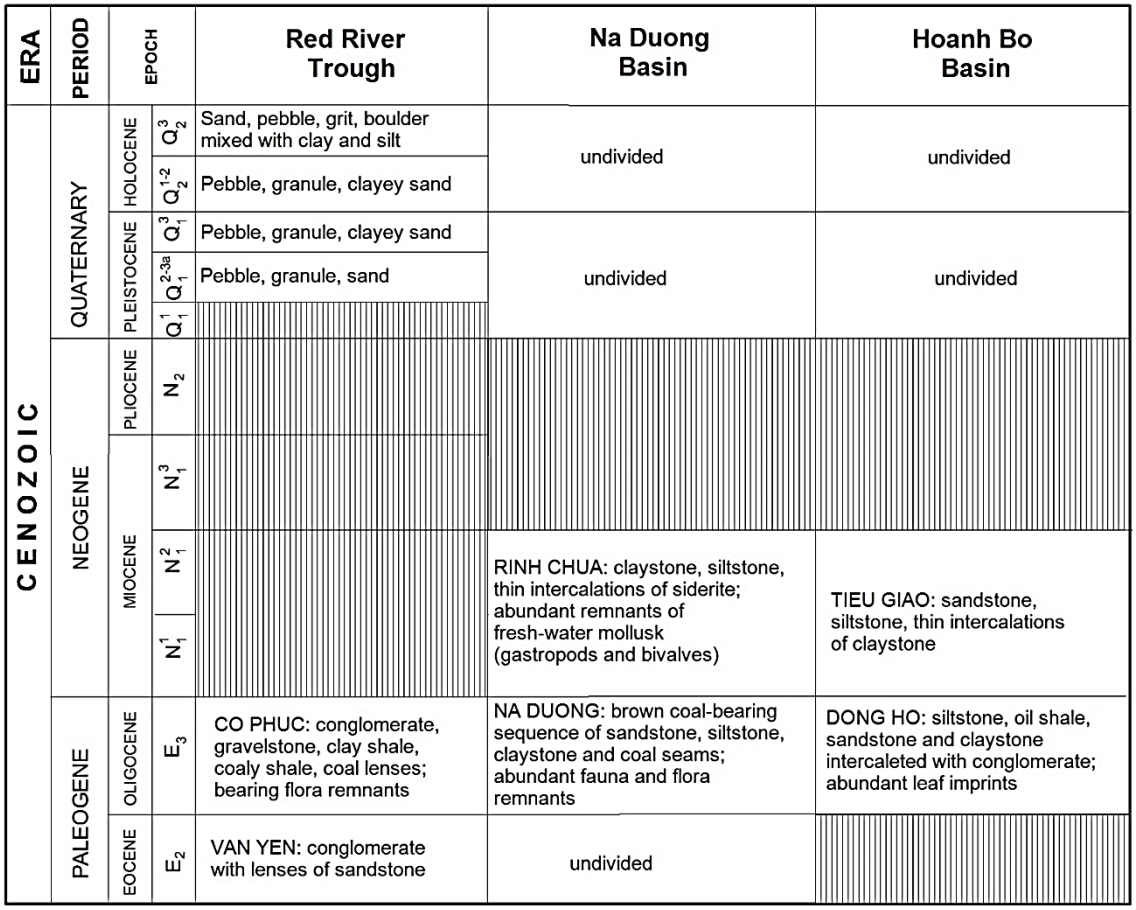

Figure 3. Stratigraphic scheme of the study basins (based on Ky et al., 1999, 2000; Luong et al., 1999; Vinh et al., 2005)

3. Materials and methods

Samples were collected at 37 sites in three areas: the Hoanh Bo basin (Ha Long - Quang Ninh province), the Na Duong basin (Lang Son province), and the Red River trough (Yen Bai province) (Fig. 1). In the Na Duong basin, stratigraphic sampling was conducted to assess paleoclimate temporal variations (Fig. 2). The samples were analyzed using the following methods: thin section analysis (13 samples), X-ray diffraction (XRD-17 samples), and palynology with the Coexistence Approach (31 samples) (Table 1).

Thin-section petrographic analysis was conducted on sandstone and siltstone samples using polarizing microscopy. This method enables the determination of the morphology, size, and variation of sediments' framework and mineral components, as well as their grain-size parameters. Paleoclimate can be inferred from these parameters, particularly the composition of quartz, feldspar, and lithic fragments (Suttner et al., 1981; Weltje et al., 1998).

XRD analysis of siltstone and claystone samples was carried out by using an Ampreean -PANanlytical Diffractometer (Cu-Kα-radiation, 45 kV, 40 mA). This method determines the percentages of clay minerals in sediments, including illite, kaolinite, chlorite, and smectite. These minerals can reflect weathering conditions, temperature, and precipitation patterns (Ducloux et al.,

1976; Meunier et al., 1980; Chamley, 1989; Vanderaveroet, 2000). Additionally, the ratios of these minerals, such as kaolinite/smectite, kaolinite/(illite+chlorite), and (kaolinite+smectite)/(illite+chlorite) can serve as indicators of humid/dry and hot/cold conditions (Adatte et al., 2002; Thamban and Rao, 2005).

Table 1. Analyzed samples

Basin	Site	Coordinates	Thin section	XRD	Palynology	Note
Hoanh Bo	#02/1	21°01'35"N; 106°59'01"E	TH02/1			Top-down sampling
	#02/2			R02/2	BTP02/2	
	#02/4				BTP02/4	
	#03/4	21°01'31"N; 106°59'04"E	TH03/4	R03/4	BTP03/4	
	#04/1	21°01'32"N; 106°59'56"E	TH04/1			
Na Duong	#05/1	21°42'40"N; 106°58'02"E		R05/1	BTP05/1	Top-down sampling
	#05/2				BTP05/2	
	#05/3			R05/3	BTP05/3	
	#05/4		TH05/4	R05/4	BTP05/4	
	#05/5				BTP05/5	
	#06/1	21°42'20"N; 106°58'06"E		R06/1	BTP06/1	Top-down sampling
	#06/2		TH06/2		BTP06/2	
	#06/3				BTP06/3	
	#06/4			R06/4	BTP06/4	
	#07/1	21°42'36"N; 106°58'18"E		R07/1	BTP07/1	Top-down sampling
	#07/2			R07/2	BTP07/2	
	#07/3			R07/3	BTP07/3	
	#07/4		TH07/4		BTP07/4	
	#08/1	21°42'35"N; 106°58'10"E			BTP08/1	
	#09/1	21°42'34"N; 106°58'17"E	TH09/1	R09/1	BTP09/1	
	#10/1	21°42'27"N; 106°56'30"E	TH10/1		BTP10/1	
Red River Trough	#13/1	21°39'56"N; 104°53'42"E	TH13/1			Top-down sampling
	#13/2				BTP13/2	
	#13/3				BTP13/3	
	#15/1	21°43'25"N; 104°50'51"E	TH15/1			
	#16/1	21°41'55"N; 104°50'43"E			BTP16/1	Top-down sampling
	#16/3				BTP16/3	
	#17/1	21°44'02"N; 104°50'12"E	TH17/1	R17/1		
	#19/1	21°46'54"N; 104°41'04"E	TH19/1	R19/1	BTP19/1	Top-down sampling
	#19/2			R19/2	BTP19/2	
	#21/1	21°47'46"N; 104°45'47"E		R21/1	BTP21/1	Top-down sampling
	#21/2				BTP21/2	
	#23/1	21°50'34"N; 104°43'11"E			BTP23/1	Top-down sampling
	#23/2			R23/2	BTP23/2	
	#24/1	21°53'19"N; 104°39'19"E		R24/1	BTP24/1	Top-down sampling
	#24/2		TH24/2			
	#25/1	21°55'19"N; 104°36'24"E			BTP25/1	
Total	**37**		**13**	**17**	**31**	

Palynological analysis was employed to identify pollen and spores in samples using an optical microscope at a magnification of 400 to 1000x. The paleoclimate is determined using the CA, which assumes that fossil plant taxa have similar climatic requirements to their nearest living relatives (NLRs). The objective of the CA is to identify the climatic interval in which all NLRs of the fossil flora can coexist (Mosbrugger and Utescher, 1997). In a given sample, a set of identified taxa A = {A1, A2, ..., An} corresponds to a set of NLR's B = {B_1, B_2, ., $B_{n.}$}. Each taxon B_i can thrive within a climate interval ($B_{i\ min}$, $B_{i\ max}$).

Using the CA, the climate interval (A_{min}, A_{max}) for the coexistence of all taxa A_i in the sample can be determined as follows:

$$A_{min} = Max\ (A'_{1\ min}, A'_{2\ min}, . ., A'_{n\ min})$$

$$A_{max} = Min\ (A'_{1\ max}, A'_{2\ max}, . ., A'_{n\ max})$$

The CA is based on the presence of taxa rather than their abundance, and its reliability increases with a higher number of analyzed taxa, typically 10 or more (Mosbrugger and Utescher, 1997). The CA commonly considers the following climatic parameters: Mean Annual Temperature (MAT), Coldest Month Temperature (CMT), Warmest Month Temperature (WMT), Mean Annual Precipitation (MAP), Highest Month Precipitation (HMP), Lowest Month Precipitation (LMP) and Warmest Month Precipitation (WMP). Each parameter, determined by the climate intervals of NLRs, typically falls within a specific range of minimum and maximum values. Therefore, it is necessary to establish their NLRs to determine the paleoclimatic conditions and identify fossil taxa through palynological analysis as described above. Climate conditions for the NLRs at the genus or family level are primarily sourced from published works (Mosbrugger and Utescher, 1997; Pross et al., 2001; Jiménez-Moreno et al., 2010; Yao et al., 2011; Quan et al., 2012; Utescher et al., 2014; Grimm et al., 2016) as well as the paleoflora database of the Steinmann Institute - University of Bonn (http://www.palaeoflora.de).

The *Köppen - Geiger climate classification* system, based on seasonal precipitation and temperature patterns, divides world climates into five groups: A (tropical), B (dry), C (temperate), D (continental), and E (polar) (Köppen, 1884; Geiger, 1954; Neck et al.,2018) (Figure). Currently, the climates in Vietnam belong to groups A and C, with northern Vietnam characterized on the world climate map as the hot monsoonal subtropical (Cwa) and monsoonal subtropical highland (Cwb) climates of group C (Beck et al., 2018). The paleoclimate of Vietnam may be related to certain climates in groups A and C. Group A climates have an average temperature of 18°C or higher throughout the year. They can be further distinguished by the following precipitation: Tropical rainforest (Af), characterized by monthly average rainfall of at least 60 mm in all months of the year; Tropical monsoon (Am), with a LMP of less than 60 mm but at least equal to the threshold (100- MAP/25); and Savanna climate (Aw), characterized by a pronounced dry season in winter, with the LMP also being less than 60 mm and below the threshold (100- MAP/25).

Group C has a CMT ranging from 0 to 18°C, with at least one month having an average temperature above 10°C. Within this group, in terms of precipitation for the studied area, two notable classifications are the dry-winter or monsoon climate (Cw) and the climate without a dry season, often called the wet climate (Cf). The climate is classified as monsoon if the HMP during the summer is at least ten times higher than the LMP in winter or if the precipitation of the six hottest months accounts for at least 70% of the MAP. For temperature classification, it is essential to differentiate between hot summer (Ca), characterized by a CMT above 0°C, at least one month's average temperature exceeding 22°C, and at least four months with an average temperature above 10°C, warm summer (Cb), where the monthly temperature are similar to those of hot summer. Still, all months have an average temperature below 22°C.

The paleoclimatic types of the studied area are primarily determined by climate parameters derived from NLR using CA, as previously mentioned. A climate that belongs to group A has a minimum CMT ≥ 18°C. Specifically, it is classified as tropical rainforest (Af) if the minimum LMP ≥ 60 mm, tropical monsoon (Am), or savanna (Aw) if the maximum LMP < 60mm. In the latter case, Am or Aw is defined based on whether it is above or below the 100 - (average MAP/25) threshold. A climate that belongs to group C has a CMT

between 0°C and 18°C. In more detail, it is classified as a hot subtropical climate (Ca) if the minimum WMT ≥ 22°C. Seasonality is determined by the ratio between the mean HPM and the mean LPM, expressed as follows:

$$HPM/LPM = ((HPM_{max} + HPM_{min})/2)/((HPM_{max} + HPM_{min})/2) = (HPM_{max} + HPM_{min})/((HPM_{max} + HPM_{min})$$

A climate is humid subtropical (Cf) if this value is below 10, or monsoon subtropical (Cw) if vice versa.

The present climates recorded at the stations of Bai Chay (Ha Long), Lang Son, and Yen Bai, located near the sampling sites in the Hoanh Bo, Na Duong basins and the Red River Trough, respectively, have MAT of 23.3°C, 21.3°C and 23°C, and MAP of 1923 mm, 1318 mm and 1961 mm (QCVN 02:2022/NXD). In the studied area, the current climate is characterized by three cold months (December, January, and February) with temperatures below 18°C, while the CMT remains above 10°C. Additionally, there are seven hot months(from April to October) with the WMT ranging from 27.1°C to 28.6°C. The ratios between the HMP in August and the LMP in December or January are 23.9 at Bai Chay, 9.8 at Lang Son, and 12.2 at Yen Bai. Based on these temperature and precipitation parameters, the present climates in the Hoanh Bo basin and Red River Trough exhibit a hot, dry-winter, subtropical monsoon climate (Cwa). In contrast, the Na Duong basin experiences a hot humid subtropical (Cfa). However, in the Na Duong basin, seasonality is somewhat indicated by an HMP/LMP ratio approximating the humid/monsoonal threshold.

4. Results

4.1. Thin section analysis

Thin-section petrographic analysis was applied to sandstone and siltstone (Fig. 4). All analyzed samples fall within coarse to very fine-grained sandstones and coarse to fine siltstones. The majority of these samples are poorly to moderately sorted. However, some are moderately well sorted (Table 2).

In sandstones, framework components account for 70-90% and are primarily composed of quartz (Q - average 34%), lithic fragments (L-average 13%), and a minor amount of feldspar (F < 6%), except sample TH24/2, which contains 18.79% of feldspar (Table 3). Siltstones exhibit framework components comprising 47-74%, predominantly quartz (average 49%), small mica and organic matter proportions, and minimal feldspar and rock fragments. The matrix is primarily clay, although iron oxides/hydroxides or sericite constitute significant proportions in some samples.

Table 2. Grain size analysis in thin section

Sample	**Classification of fine-grained deposits (Picard 1971)**	**Sorting of framework composition**	**Size range** (mm)
TH02/1	Coarse sand	Moderately sorted	0.063-0.94
TH24/2	Medium sandstone	Moderately well sorted	0.063-0.69
TH04/1	Medium sandstone	Poorly to moderately sorted	0.063-0.27
TH09/1	Fine sandstone	Poorly to moderately sorted	0.063-0.135
TH05/4	Fine sandstone	Moderately well sorted	0.063-0.129
TH03/4	Very fine sandstone	Moderately sorted	0.063-0.10
TH17/1	Sandy siltstone	Poorly to moderately sorted	0.004-0.068
TH06/2	Siltstone	Moderately well sorted	0.004-0.044
TH19/1	Coarse siltstone	Poorly to moderately sorted	0.004-0.053
TH10/1	Coarse siltstone	Poorly to moderately sorted	0.004-0.042
TH15/1	Medium siltstone	Moderately well sorted	0.004-0.033
TH07/4	Fine siltstone	Poorly to moderately well sorted	0.004-0.015

Note: Sorting is based on textural comparison charts after Folk (1968) and Longiaru (1987)

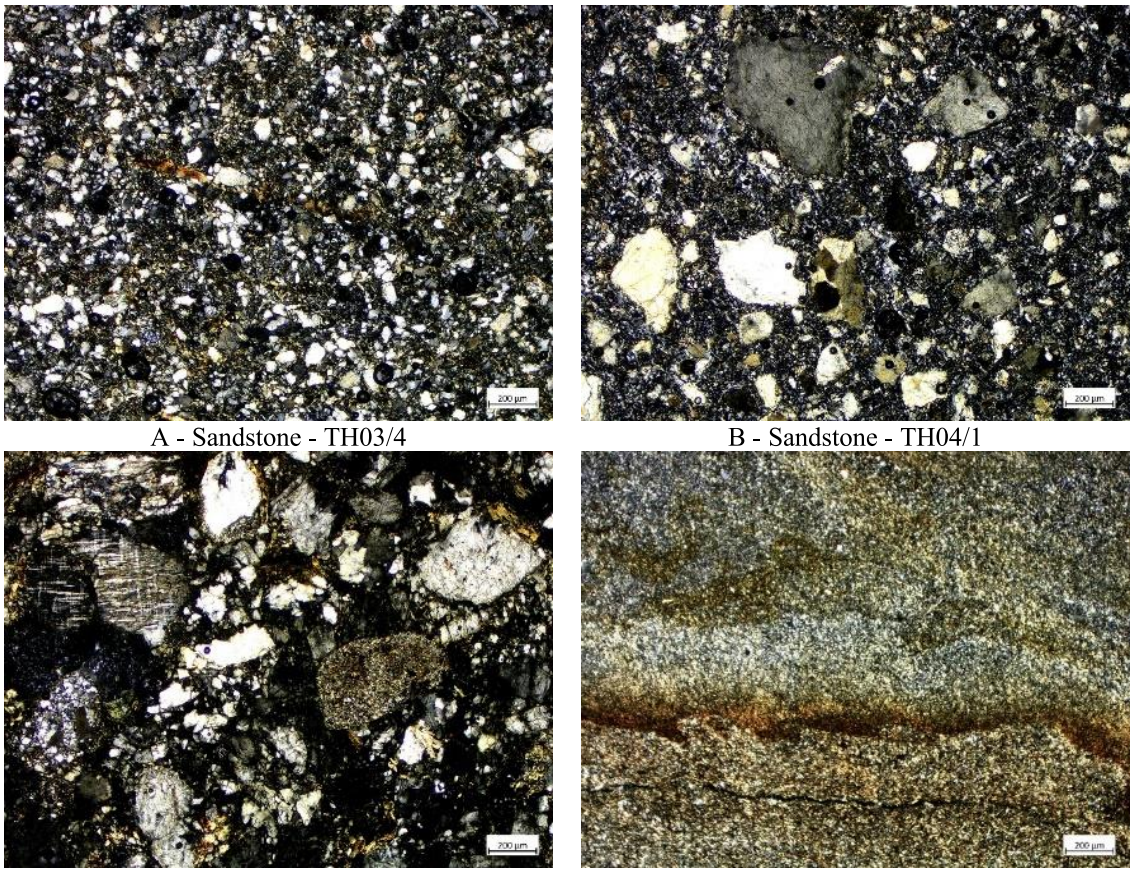

A - Sandstone - TH03/4 B - Sandstone - TH04/1

C - Sandstone - TH24/2 D- Siltstone - TH15/1

Figure 4. Thin section of sandstones and siltstone (scale = 200 μm)

Table 3. Essential components (%) of sedimentary rocks in thin section

	Sample	Framework components									Matrix cements/diagenetic minerals
		Q	F	L	Others					∑ FC	
					Micas	Opaque minerals	OM	Heavy minerals	NR		
Sandstone	TH02/1	20.72	3.70	27.13	0.00	0.00	0.00	0.00	18.00	69.55	30.45
	TH03/4	52.91	2.95	4.35	4.82	0.00	1.20	0.00	18.81	85.04	14.96
	TH04/1	34.40	5.56	25.55	0.00	0.39	0.00	0.00	3.57	69.47	30.53
	TH05/4	39.12	2.31	10.01	0.69	0.00	4.86	0.00	15.29	72.28	27.72
	TH09/1	40.74	2.66	5.67	0.46	0.00	0.00	0.00	22.46	71.99	28.01
	TH24/2	17.73	18.79	7.91	2.69	0.00	0.00	0.38	41.63	89.13	10.87

	Sample	Framework components					Matrix cements/diagenetic minerals				
		Q.	Micas	OM	NR	∑ FC	Clay	Fe	Clay-Fe	Sericite	∑ C
Siltstone	TH06/2	47.21	10.50	1.85	8.24	67.80	26.70	0.00	0.00	5.50	32.20
	TH07/4	53.72	3.47	0.00	0.00	57.19	12.03	0.00	0.00	30.78	42.81
	TH10/1	56.71	11.51	6.08	0.00	74.30	25.70	0.00	0.00	0.00	25.70
	TH15/1	50.10	13.21	0.00	0.00	63.31	23.00	4.59	8.10	1.00	36.69
	TH17/1	52.50	5.70	7.14	0.00	65.34	5.93	16.46	12.27	0.00	34.66
	TH19/1	33.59	2.78	10.41	0.00	46.78	15.50	0.00	0.00	37.72	53.22

Note: Q - quartz, F- feldspar, L-lithic fragments, OM-organic matters, NR- nonrecognizable

4.2. XRD analyses

The XRD method was used to analyze the claystone samples (Fig. 5). The mineral components of these samples are primarily quartz (21-78%, avg. 43%), illite (6-56%, avg. 33%), and kaolinite (3-28%, avg. 11%). Other minerals, such as chlorite, feldspar, and smectite, are also quite common. In particular, some samples present siderite, goethite, calcite, and ankerite in relatively high proportions (Table 4).

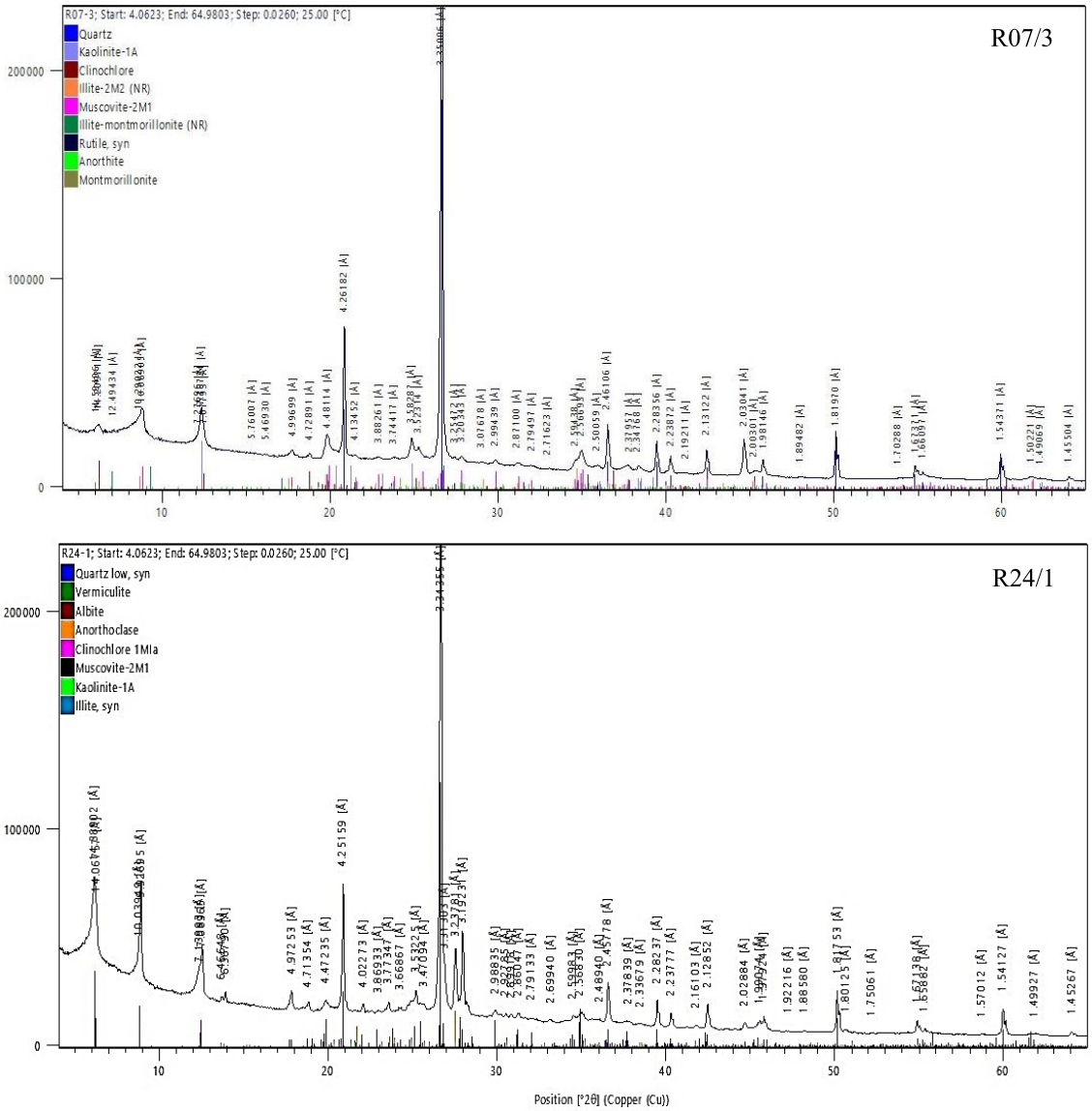

Figure 5. XRD analysis of claystones

Table 4. Mineral percentage in claystone

Sample	Quartz	Illite	Kaolinite	Chlorite	Feldspar	Smectite	Others
R02/2	78	7	14				Pyrolusite -1, Pyrophyllite<1, Calcite<1
R03/4	65	6	25		2		Anatase -<1, Pyrite <1, Pyrophylit2-2
R05/1	35	35	16	3		10	Vermiculite-1
R05/3	47	40	10	2			Anatase <1, Magnetite-1
R05/4	73	15	4				Pyrite <1, Gypsum-2, Ankerite-6
R06/1	41	42	12	5			
R06/4	53	32	11	4			
R07/1	36	47	11	5			Anatase -1
R07/2	31	11	13	3			Siderite-34, Calcite-8,
R07/3	34	29	12	6	2	16	Rutile-1
R09/1	61	28	10				Vermiculite <1, Pyrochroite-1
R17/1	37	46	9				Goethite-8,
R19/1	34	56	3			7	
R19/2	34	51	4	6	5		Rutile<1
R21/1	24	38	28				Goethite-10
R23/2	21	39	4	13	16		Pyrite <1, Dolomite-3, Rutile-1, Calcite-3
R24/1	26	35	4	7	26		Vermiculite-2

4.3. Pollen and spores in samples and their NLRs

Pollen and spores are present in 17 samples, representing 55% of the total, collected from the Na Duong basin and the Red River trough (Fig. 6). No palynomorphs were found in any of the samples taken from the Hoanh Bo basin.

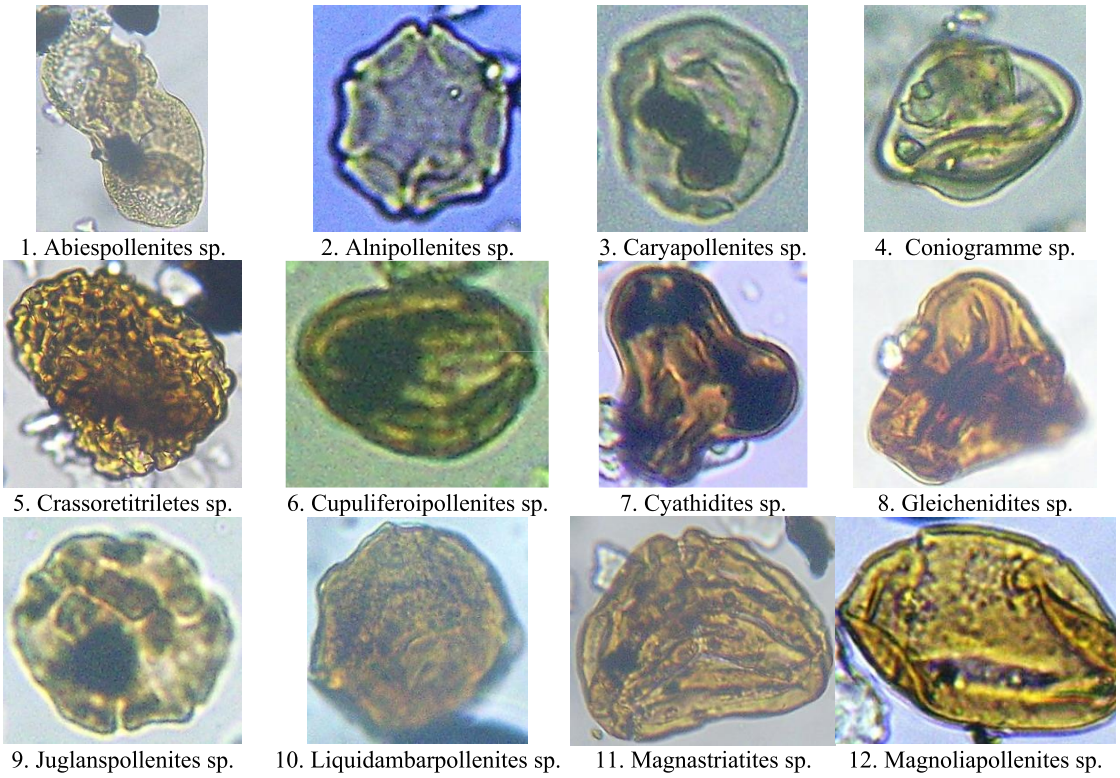

1. Abiespollenites sp. 2. Alnipollenites sp. 3. Caryapollenites sp. 4. Coniogramme sp.
5. Crassoretitriletes sp. 6. Cupuliferoipollenites sp. 7. Cyathidites sp. 8. Gleichenidites sp.
9. Juglanspollenites sp. 10. Liquidambarpollenites sp. 11. Magnastriatites sp. 12. Magnoliapollenites sp.

Figure 6. Typical palynomorphs in samples taken from Na Duong basin and Red River Trough


13. Moruspollenites sp.


14. Myricipites sp.


15. Phragmites sp.

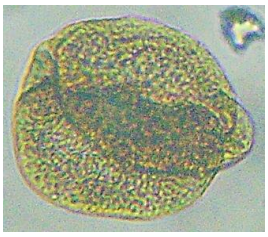
16. Pinuspollenites sp.


17. Plagiogyria sp.


18. Platycaryapollenites sp.

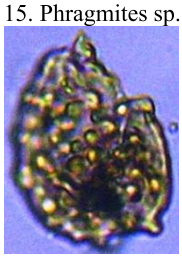
19. Stenochlaenla sp.

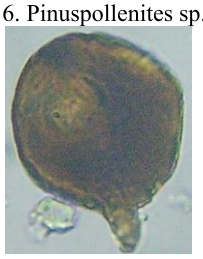
20. Sequoiapollenites sp.


21. Tricolporopollenites sp.

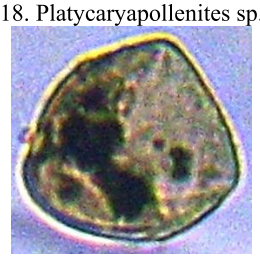
22. Triporopollenites sp.

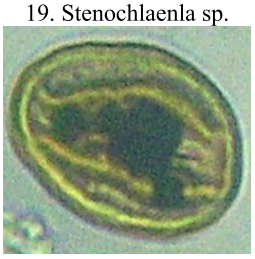
23. Quercoidites sp.


24. Verucatosporites sp.

Figure 6. Cont.

For the Na Duong basin, palynomorphs were identified in 12 samples, arranged from top to bottom in the cross section as follows:

- BTP-05/1: Verucatosporites sp., Cyathidites sp., Lygodiumsporites sp., Crassoretitriletes sp., Quercoidites sp., Platycaryapollenites sp., Cupuliferoipollenites sp., Phragmites sp., Abiespollenites sp., Pinuspollenites sp., Stenochlaenla sp.
- BTP-05/2: Pteris sp., Verucatosporites sp., Gleichenidites sp., Caryapollenites sp., Tricolporopollenites sp., Platycaryapollenites sp., Stenochlaenla sp. Magnoliapollenites sp., Crassoretitriletes sp., Poaceae gen. indet., Quercoidites sp.
- BTP-05/3: Lycopodiumsporites sp., Abiespollenites sp., Pinuspollenites sp., Stenochlaenla sp., Rhus sp., Juglanspollenites sp., Moruspollenites sp.
- BTP-05/4: Poaceae gen. indet., Crassoretitriletes sp., Quercoidites sp., Platycaryapollenites sp., Triporopollenites sp., Magnastriatites sp.
- BTP-05/5: Verucatosporites sp., Pteris sp., Lycopodiumsporites sp., Osmunda sp., Caryapollenites sp., Platycaryapollenites sp., Pinuspollenites sp., Quercoidites sp., Pinuspollenites sp.
- BTP-06/1: Crassoretitriletes sp., Verucatosporites sp., Pinuspollenites sp., Pterocaryapollenites sp., Quercoidites sp., Triporopollenites sp., Gramineae gen. indet., Phragmites sp.
- BTP-06/2: Crassoretitriletes sp., Quercoidites sp., Platycaryapollenites sp., Abiespollenites sp., Pinuspollenites sp., Tricolporopollenites sp.
- BTP-06/3: Platycaryapollenites sp., Pinuspollenites sp., Crassoretitriletes sp., Quercoidites sp., Triporopollenites sp., Gramineae gen. indet.
- BTP-06/4: Verucatosporites sp., Osmunda sp., Lycopodiumsporites sp.,

Abiespollenites sp., Crassoretitriletes sp., Quercoidites sp., Platycaryapollenites sp., Tiliaephylum sp.,

- BTP-07/1: Crassoretitriletes sp., Cyathidites sp., Quercoidites sp., Triporopollenites sp., Poaceae gen. indet.

- BTP-08/1: Verucatosporites sp., Ceratopteris sp., Liliaceae gen. indet., Crassoretitriletes sp., Quercoidites sp., Platycaryapollenites sp., Liquidambarpollenites sp., Cupuliferoipollenites sp.

- BTP-10/1: Verucatosporites sp., Coniogramme sp., Plagiogyria sp., Myricipites sp., Quercoidites sp., Caryapollenites sp., Poaceae gen. indet., Sequoiapollenites sp.

In the Red River trough five samples were collected from the Co Phuc Formation, and the results for these samples are as follows:

- BTP 13/3: Crassoretitriletes sp., Verucatosporites sp., Cyathidites sp., Plagiogyria sp., Poaceae gen. indet.

- BTP-19/1: Verucatosporites sp., Plagiogyria sp., Crassoretitriletes sp., Cyathidites sp., Myricipites sp., Cupuliferoipollenites sp., Quercoidites sp., Gramineae gen.indet.

- BTP-21/2: Lycopodiumsporites sp., Verucatosporites sp., Pteris sp., Caryapollenites sp., Pinuspollenites sp., Faguspollenites sp., Alnipollenites sp.

- BTP-23/2: Lygodium sp., Verucatosporites sp., Crassoretitriletes sp., Pterocaryapollenites sp., Quercoidites sp., Juglanspollenites sp., Rhus sp.

- BTP-24/1: Crassoretitriletes sp., Verucatosporites sp., Poaceae gen. indet., Pinuspollenites sp., Quercoidites sp.

The pollen and spores identified in the 17 samples belong to 37 taxa, of which 31 can be quantified for paleoclimate using their NLRs (Table 5). The suitable temperature and precipitation for the taxa in the fossil floras are determined based on the current climatic conditions in the regions where their NLRs are distributed.

Table 5. Taxa identified in samples, their NRLs and climatic parameters

#	Fossil taxon	NLR	MAT (°C)		MAP (mm)		CMT (°C)		WMT (°C)		HMP (mm)		LMP (mm)		WMP (mm)	
			Min	Max	Min	Max	Min	Max	Min	Max	Min	Max	Min	Max	Min	Max
1	Abiespollenites sp.	Abies sp.	-6.9	21.7	373	2648	-24.4	25.6	13.8	29.5	57	369	0	70	0	344
2	Alnipollenites sp.	Alnus sp.	-13.3	27.4	41	2559	-40.9	25.6	12	38.6	8	353	0	135	8	207
3	Caryapollenites sp.	Carya sp.	4.4	26.6	373	1724	-11.5	22.2	19.3	30.6	68	434	8	70	45	258
4	Coniogramme sp.	Adiantaceae	-4.9	27.7	-	-	-	-	-	-	-	-	-	-	-	-
5	Crassoretitriletes sp.	Lygodium sp.	9.3	27.1	1122	2845	-2.8	25.6	21.6	29.8	115	349	19	157	68	217
6	Cupuliferoipollenites sp.	Castanea sp.	8.7	24.2	473	1857	-3.9	16.7	21.6	29.4	70	424	3	88	3	239
7	Cyathidites sp.	Cyatheaceae	15.2	27.7	1035	3151	6.6	27	19.6	28.1	134	454	12	165	93	224
8	Faguspollenites sp.	Fagus sp.	4.4	23.1	422	2100	-11.5	17	17.3	28.5	46	448	5	94	5	431
9	Gleicheniidites sp.	Gleichenia sp.	13.5	27.1	1183	2559	1.8	23	25.4	29.9	205	448	3	135	85	431
10	Juglanspollenites sp.	Juglans sp.	0	27.5	210	2617	-22.7	25	13.7	31.2	44	582	1	114	2	189
11	Liquidambarpollenites sp.	Liquidambar sp.	11.5	24.6	619	1823	-1	23.8	23	29.3	109	340	2	72	5	195
12	Lycopodiumsporites sp.	Lycopodiaceae	-6.7	16.5	177	1958	-25.6	7.1	13.8	27.4	27	294	2	83	10	189
13	Magnastriatites sp.	Schizaeaceae	2	27.7	705	3151	-12.8	27	13.5	28.2	84	454	6	165	82	269
14	Magnoliapollenites sp.	Magnolia sp.	6.2	27	578	3500	-10.2	25.9	19.6	28.6	102	610	1	180	70	462

#	Fossil taxon	NLR	MAT (°C)		MAP (mm)		CMT (°C)		WMT (°C)		HMP (mm)		LMP (mm)		WMP (mm)	
			Min	Max	Min	Max	Min	Max	Min	Max	Min	Max	Min	Max	Min	Max
15	Moruspollenites sp.	Morus sp.	3.1	21.9	305	1722	-11.8	13.6	15.6	28.9	82	292	0	83	82	264
16	Myricipites sp.	Myrica sp.	-6.9	28.1	233	3151	-25	27	8.9	33.9	51	389	0	165	0	221
17	Osmunda sp.	Osmundaceae	0.2	23.9	206	1864	-16.6	19.4	16.3	29.5	34	289	2	59	2	228
18	Laevigatosporites sp.	Polypodiaceae	-4.9	22.2	224	2336	-32.4	16.6	18.2	28.5	43	454	0	75	0	269
19	Plagiogyria sp.	Plagiogyriaceae	4.3	28.6	185	3230	-1.7	22.3	13.9	35.2	61	420	4	165	42	221
20	Platycaryapollenites sp.	Platycarya sp.	6.9	23.1	378	1812	-6.4	17	18.3	28.8	92	431	1	37	73	431
21	Pinuspollenites sp.	Pinus sp.	-9.2	25.5	180	1741	-36.8	21.4	7.1	32.9	28	293	0	94	0	304
22	Pteris sp.	Pteris sp.	2	21.7	705	2336	-12.8	14.8	13.5	28.2	84	454	6	95	82	269
23	Pterocaryapollenites sp.	Pterocarya sp.	7	24.2	246	2648	-6.5	16.4	17.7	31.6	46	424	1	64	2	424
24	Quercoidites sp.	Quercus sp.	0	27	201	3905	-22.7	25.9	13.7	28.3	33	610	5	180	5	180
25	Rhus sp.	Rhus sp.	3.4	24.9	735	1613	-12.9	22.2	18.9	29.4	73	195	18	93	49	195
26	Sequoiapollenites sp.	Sequoia sempervirens	9.4	15.3	-	-	-	-	-	-	-	-	-	-	-	-
27	Stenochlaenla sp.	Blechnaceae	9.3	27.1	1122	2845	-2.8	25.6	21.6	29.8	115	349	19	157	68	217
28	Tiliaephylum sp.	Tilia sp.	2.5	20.8	373	1958	-17.7	13.3	15	28.1	68	236	9	83	45	195
29	Tricolporopollenites sp.	Castanopsis sp.	9.3	27.9	397	3151	-1.5	27	20	32.5	70	610	5	165	5	366
30	Triporopollenites sp.	Corylus sp.	-4.9	24	389	1682	-32.4	16.7	12.9	29.4	45	343	3	73	3	239
31	Verucatosporites sp.	Polypodium sp.	-4.9	27.7	-	-	-	-	-	-	-	-	-	-	-	-

Note: "-"means "not available data"

Synthetized from Mosbrugger and Utescher, 1997; Pross et al., 2001; Jiménez-Moreno et al., 2010; Yao et al., 2011; Quan et al., 2012; Utescher et al., 2014; Grimm et al., 2016 and http://www.palaeoflora.de

5. Discussions

5.1. Stratigraphy and sedimentary environments

In the Hoanh Bo basin, no palynomorphs have been identified in the analyzed samples. However, the Dong Ho Formation in this basin has been assigned to the Oligocene epoch based on the presence of an assemblage that includes Pentapollenites maoningensis, Cicatricosisporites dorogensis, Verrutricolporites pachydemus, Gothanipollis bassensis, Liquidambarpollenites minutus, Lycopodiumsporites neogenicus (Trung et al., 1999). The sediments of this formation comprise conglomerate, gritstone, sandstone, siltstone and claystone, interbedded with thin layers of coaly shale oil shale (Luong et al., 1999, Ky et al., 1999). These sediments were deposited in alluvial fan, alluvial plain, fluvial and lacustrine environments (Tha et al., 2017; Wysoka et al., 2022).

In the Na Duong basin, samples taken from a cross-section of Na Duong Formation revealed a palynomorph assemblage consisting of Verucatosporites sp., Cyathidites sp., Stenochlaenla sp.; Crassoretitriletes sp., Magnastriatites sp.; Lycopodiumsporites sp., Coniogramme sp., Plagiogyria sp., Pteris sp., Gleichenidites sp. Quercoidites sp., Caryapollenites sp., Myricipites sp., Platycaryapollenites sp., Cupuliferoipollenites sp., Tricolporopollenites sp. Rhus sp., Juglanspollenites sp.; Moruspollenites sp., Phragmites sp., Magnoliapollenites sp., Poaceae gen. indet., Triporopollenites sp.,

Liquidambarpollenites sp., Abiespollenites sp., Pinuspollenites sp., Sequoiapollenites sp. The spore-pollen spectra indicate 25-50%, 5-20% and 30-70% for spores, gymnosperm and angiosperm, respectively. The vegetation is dominated by deciduous broad-leaved forests, featuring genera such as Carya, Castanea, Corylus, Juglans, Liquidambar, Magnoliapollenites, Morus, Platycarya, Pterocarya and Quercus, sometimes intermixed with coniferous forests represented by Abies, Pinus and Sequoia, or with evergreen ferns such as Cyathea. The dating of the spore-pollen assemblages in the Na Duong basin and Red River trough is based on palynological results from Cenozoic basins in Southeast Asia and Vietnam (Bat et al., 2008). The First Appearance Datum (FAD) in the Oligocene includes Magnastriatites sp., Stenochlaenla sp., and Crassoretitriletes sp. On the other hand, the Last Appearance Datum (LAD) for the Oligocene includes Cicatricosisporites sp., Lycopodiumsporites sp., and Verucatosporites sp. A typical palynomorph assemblage found in Paleogene sediments in southern China consists of Myricipites sp., Quercoidites sp., Caryapollenites sp., Cupuliferoipollenites sp., Faguspollenites sp., Tricolporopollenites sp., Alnipollenites sp., Juglanspollenites sp., Rhus sp., and Pinuspollenites sp. (Song, 1996). Based on these findings, the palynomorph assemblages in the Na Duong formation may indicate an Oligocene age. Böhme et al. (2013) suggested an Eocene age for this formation based on mammal fossils, mainly two species: Bakalovia orientalis nov. sp. (Anthracotheriidae) and Epiaceratherium naduongense nov. sp. (Rhinocerotidae),. However, all known pollen assemblages with Middle-Late Eocene features from Southern China are absent from the Na Duong and Rinh Chua formations. Moreover, the Early Oligocene could be assigned for these two formations based on a comparison of their pollen assemblages with those from other sedimentary basins located in the Red River Fault Zone, such as the Nanning, Ningming, Maoming, and Cao Bang Basins (Wysoka et al., 2020). Thus, from a palynological perspective, the Na Duong formation could be dated as Oligocene. This formation is characterized by coaly shale, siltstone, sandstone, seam, and lignite lenses deposited in fluvial and lacustrine environments.

A palynomorph assemblage in the Red River Trough is present, comprising Verucatosporites sp., Coniogramme sp. Crassoretitriletes sp., Cyathidites sp., Lycopodiumsporites sp., Plagiogyria sp., Myricipites sp., Quercoidites sp., Caryapollenites sp., Poaceae gen. indet., Cupuliferoipollenites sp., Faguspollenites sp., Alnipollenites sp., Juglanspollenites sp., Rhus sp., Pinuspollenites sp. The spore-pollen spectra reveal the following percentages: 10-50% spores, 0-20% gymnosperm pollen and 30-80% angiosperm pollen. The vegetation is predominantly characterized by deciduous broad-leaved forests, with genera such as Castanea, Alnus, Carya, Fagus, Juglans, Pterocarya and Quercus, possibly mixed with needle-leaved forests of Pinus or with evergreen tree fern of the genus Cyathea. Lygodium, Polypodiaceae, Plagiogyria, and Poaceae also represent herbaceous vegetation. Pollen assemblages in the Co Phuc formation, similar to Na Duong formation, indicate an Oligocene age. This conclusion is based on several key events: the Oligocene FAD of Magnastriatites sp., Stenochlaenla sp., and Crassoretitriletes sp.; the Oligocene LAD of Cicatricosisporites sp., Lycopodiumsporites sp. and Verucatosporites sp.; the Paleogene assemblage in southern China includes taxa such as Myricipites sp., Quercoidites sp., Caryapollenites sp., Cupuliferoipollenites sp., Faguspollenites sp., Tricolporopollenites sp., Alnipollenites sp., Juglanspollenites sp., Rhus sp., and Pinuspollenites sp. (Song, 1996). The

Co Phuc Formation consists of conglomerate, gravelstone, clay shale, coal shale, and coal lenses (Vinh et al., 2005), formed in alluvial fan and lacustrine environments (Huyen et al., 2004).

5.2. Paleoclimate interpreted from analyses of thin section and XRD

The thin-section analyzed sandstones are primarily classified as litharenite, sublitharenite, and lithic arkose (Fig. 7, Fig. 4 A, B and C). Samples from the Dong Ho and Na Duong formations, consistent with the findings of Tha et al. (2017) and Wysoka et al. (2020), show low feldspar content, categorizing them as litharenite and sublitharenite, indicating a relatively weathered solid bedrock area. The sublitharenite samples (TH03/4, TH05/4 and TH09/1) contain a relatively high quartz content, which may be indicative of a humid climate, while the litharenite samples (TH04/1 and TH02/1) may reflect drier condition (Fig. 7-right). Notably, in the lithic arkose sandstone of the sample TH24/2, feldspar is present in significant amounts (17.73%), and appears relatively fresh despite being subjected to transportation and sedimentation processes (Fig. 4). This preservation may be attributed to non-weathering conditions associated with a cold, semi-arid, sub-humid climate. According to the diagram by Suttner et al. (1981), this sample falls within the overlap of humid and semi-arid area (Fig. 7- right).

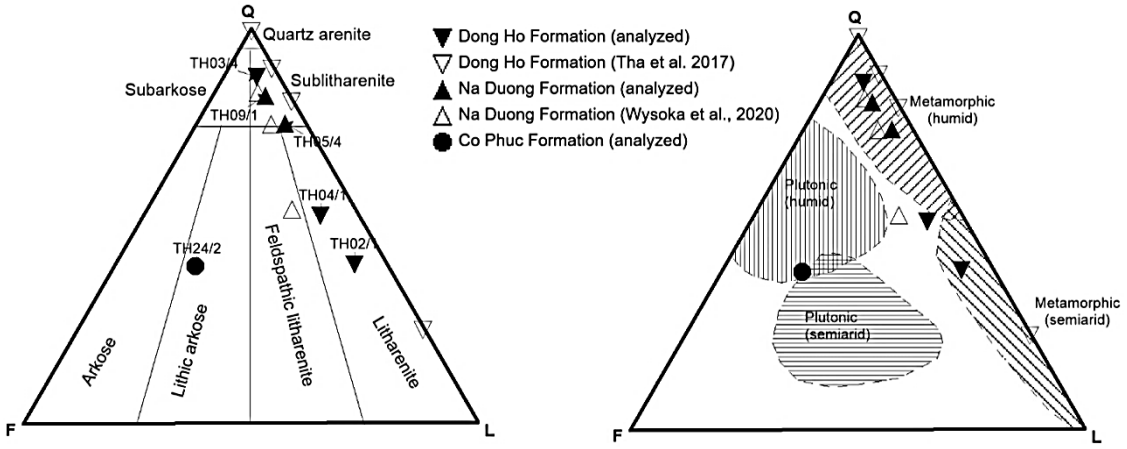

Figure 7. Ternary QFL diagram based on Folk, 1980 (left) and Suttner et al., 1981 (right)

In the bivariate plot of ln(Q/F)-ln(Q/L), the analyzed sandstones fall into the following semiquantitative weathering index (Iw): 0 (TH2/1, TH4/1 and TH24/2), 1 (TH05/4) and 2 (TH03/4 and TH09/1), corresponding to unweathered, slightly and moderately weathered conditions, respectively (Fig. 8). The Iw attempts to relate weathering to the present-day climate and physiography of sediment sources (Weltje, 1994), defined as Iw=CR, where C is a semiquantitative indicator of climate (primarily rainfall) used as a proxy for the time-averaged weathering rate, and R is a semiquantitative relief indicator assumed to be inversely proportional to the residence time in the source area. Iw is a relative value reflecting conditions such as (semi)arid climate or mountainous regions (Iw=0); the subhumid climate in hilly areas (Iw=1), the subhumid climate in plains or humid climate in hilly areas (Iw=2).

The thin-section analyses show weakly consolidated gray siltstones that do not reflect climatic conditions but are related to the rock source. In the Red River Trough, some samples (TH15/1, TH17/1, and TH19/1)

exhibit white-gray and yellow-gray mottled colors, along with a high content of iron oxide and iron-rich clay in their cement composition, which may indicate changes in humid/dry climates. The siltstone from sample TH15/1 is particularly illustrative of this phenomenon, displaying brown streaks indicative of the accumulation of iron-rich solutions resulting from the chemical weathering in a climate characterized by alternating humid and dry conditions (Fig. 4D).

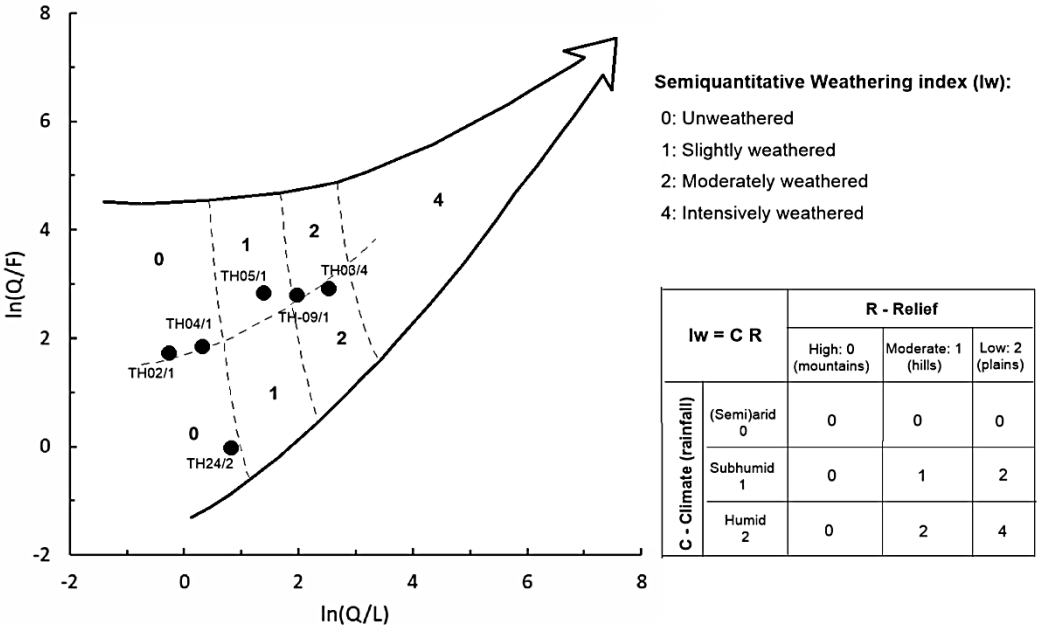

Figure 8. Bivariate log-ratio plot of sandstone, showing the relation between petrographic composition, parentage, and climatic-physiographic conditions (based on Weltje et al., 1998)

Illite and kaolinite are present in all claystone samples analyzed by XRD (Fig. 5). Illite is derived from aluminosilicate minerals, such as feldspar and mica, through weathering processes that involve the removal of K^+ ions under dry climatic conditions with limited rainfall (Meunier et al.,1980; Yan, 1988). Additionally, dry climates are favorable for the preservation of illite (Long et al., 2007). Kaolinite can be either a primary or secondary mineral. In the second case, it is produced by chemical weathering in warm, humid climates (Chamley, 1989; Velde, 1992; Naidu et al., 1995; Corenti et al., 2020) and acidic conditions (Sun et al., 2022). A warm and humid climate facilitates kaolinite formation and preservation (Chen et al., 2003; Sun et al., 2022). Chlorite, found in many samples in Na Duong and Red River Trough, forms in alkaline environments and is unstable under oxidizing conditions. Therefore, it typically survives only in areas where chemical weathering is inhibited, such as glaciers or arid surfaces (Ducloux et al., 1976). Because chlorite is unstable under warm, humid, and strongly acidic conditions, its occurrence in the samples suggests a cooler or arid weathering environment. Smectite is present in three samples from the Na Duong basin (R05/1, R07/3) and the Red River Trough (R19/1). It is often a product of chemical weathering in alkaline environments or hot, dry climates (Chamley, 1989; Velde, 1992; Naidu et al., 1995; Thiry, 2000). Smectite can also form in cold climates (Ehrmann, 1988) or under alternating wet-dry conditions (Keller et

al., 1970). The coexistence of smectite with hematite suggests a semi-arid climate (Jimenez-Espinosa et al., 2003). In contrast, illite-smectite mixed layers indicate a gradual change to a humid environment (Jain et al., 2003). Feldspar, a rock-forming mineral, undergoes chemical weathering through hydrolysis, producing clay minerals, including illite, smectite, and kaolinite. The presence of feldspar in some XRD samples (Table 4) suggests limited chemical weathering, possibly associated with cold, dry climatic conditions. Notably, in samples R23/2 and R24/1, the feldspar content is significantly higher than that of kaolinite, coupled with a high illite content, indicating a dry, cold climate (Table 4). This observation is further supported for sample R24/1 by vermiculite (2%), a mineral commonly formed under cold conditions (Li et al., 2019).

Generally, instead of relying on individual clay minerals, their assemblage and related ratios are utilized to determine weathering, temperature, and precipitation. Illite and chlorite are products of physical weathering in high-latitude, cold climates (Chamley, 1989; Velde, 1992). Increases in chlorite and illite content are commonly interpreted as indicative of climatic conditions that gradually become colder and drier (Vanderaveroet et al., 2000; Gingele et al., 2001; Sun et al., 2022). The kaolinite/smectite ratio reflects weathering properties that vary between hot and humid conditions (characterized by a dominance of kaolinite) and dry season climates (characterized by a dominance of smectite) (Adatte et al., 2002). Considering this ratio, samples R07/3 and R19/1, which exhibit smectite dominance, may be associated with cold and dry conditions; conversely, sample R05/1, which shows kaolinite dominance, indicates less dryness, possibly related to the monsoon feature (Table 6). The ratios of kaolinite/illite kaolinite/(illite + chlorite) serve as humidity indicators, with higher values suggesting increased moisture (Thamban and Rao, 2005). When these ratios are considered, samples from the Hoanh Bo basin (R02/2, R03/4) indicate hot and humid conditions with a predominance of kaolinite. In contrast, some samples from the Red River Trough (R19/1, R19/2, R23/2) display characteristics of cold and dry climates (Table). The variation in the kaolinite/smectite ratio reflects changes between hot and humid conditions (rich in kaolinite) and dry season (rich in smectite) (Adatte et al., 2002).

Table 6. Ratios of clay minerals

Sample	Kaolinite/Illite	Kaolinite/Smectite	Kaolinite/(Illite+Chlorite)	(Kaolinite+Smectite)/(Illite+Chlorite)
R02/2	2.00		2.00	2.00
R03/4	4.17		4.17	4.17
R05/1	0.46	1.60	0.42	0.68
R05/3	0.25		0.24	0.24
R05/4	0.27		0.27	0.27
R06/1	0.29		0.26	0.26
R06/4	0.34		0.31	0.31
R07/1	0.23		0.21	0.21
R07/2	1.18		0.93	0.93
R07/3	0.41	0.75	0.34	0.80
R09/1	0.36		0.36	0.36
R17/1	0.20		0.20	0.20
R19/1	0.05	0.43	0.05	0.18
R19/2	0.08		0.07	0.07
R21/1	0.74		0.74	0.74
R23/2	0.10		0.08	0.08
R24/1	0.11		0.10	0.10

5.3. Paleoclimate interpreted from palynological analyses with CA principle

The paleoclimatic parameters, including MAT, CMT, WMT, MAP, HMP, LMP, and WMP, are quantified for the 17 samples through CA using the NLR of fossil plants (Fig. 9).

In the Red River Trough, the analyzed samples indicate the MAT conditions ranging from 4.4 to 25.5°C, with the majority falling between 9.3 and 22.2°C. Except for BTP-24/1, all samples exhibit temperatures lower than the present MAT of 23°C for the region. The MAPs in samples range from 705 to 2336 mm, with most samples falling between 1122 and 1857 mm, suggesting a climate characterized by minor to moderate precipitation. Generally, these MAP values are lower than the present MAP of 1961 mm, except for sample BTP-13/3. Based on these findings, the paleoclimates inferred from the analyzed samples in the Red River Trough are generally colder and drier than the current conditions.

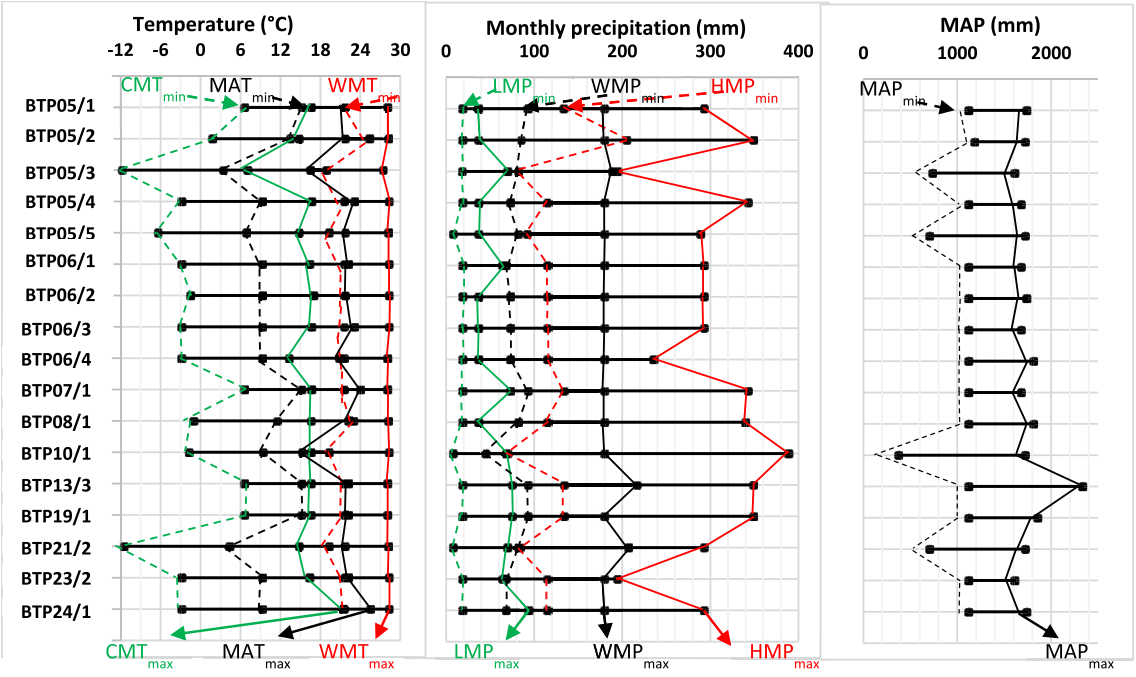

Figure 9. Paleoclimatic parameters in the samples

In the Na Duong basin, the MAT in all samples ranges from 3.4°C (lowest limit) to 24°C (highest limit), with the majority falling between 9.3 and 21.7°C. All lower thresholds are below the current MAT of 21.3°C, while most upper thresholds exceed this value by 0.4°C to 2.7°C. Notably, the maximum MATs in samples BTP-05/3, BTP-06/4, and BTP-10/1 are below the current MAT, indicating colder paleoclimates than present. The MAPs range from 373 mm to 1812 mm, with most samples falling between 1122 mm and 1724 mm, reflecting low to moderate precipitation conditions. Relatively high WMP values indicate that a significant portion of the precipitation occurs during the summer months (Fig. 9). Regarding temperature, the CMTs exhibit a wide range from -11.8°C to 16.7°C, with the majority falling between -3°C and 16°C. In contrast, the WMTs show a narrower range of 18.9°C to 28.3°C. For precipitation, the LMP values range from 8 mm to 70 mm,

while the HMP values exhibit a broader range of 82 mm to 343 mm. These variations in temperature and precipitation suggest a monsoonal climate pattern characterized by a slight distinction between cold, dry winters and hot, humid summers (Fig. 10).

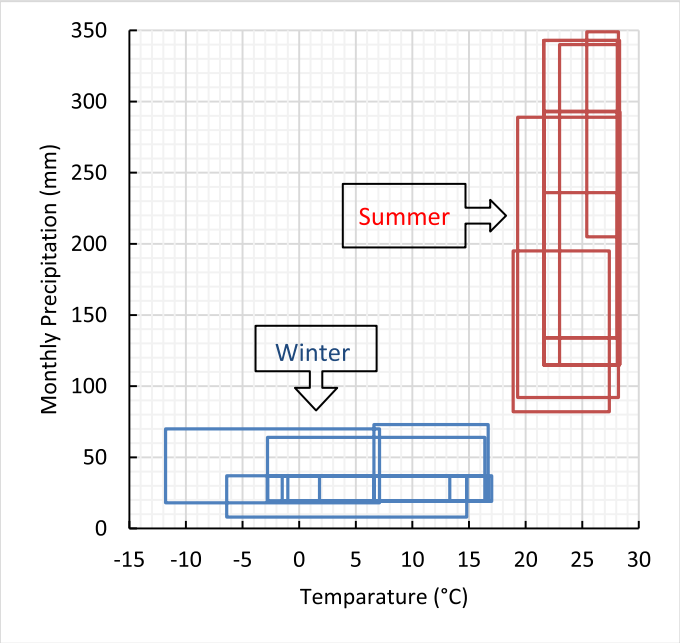

Figure 10. Seasonal temperature and precipitation in Na Duong basin

The paleoclimatic parameters in samples, except BTP24/1, fall into the temperate climate group (C), characterized by a CMT_{max} <18ºC (Fig. 9). Among these samples, two BTP-5/2 and BTP-8/1 exhibit WMT_{min} >22°C, indicating that they meet the criterion of having at least one month with temperature exceeding 22 °C, thus confirming their classification as hot subtropical climates (Ca). Due to insufficient information, it is impossible to determine whether the remaining samples specifically belong to the hot (Ca) or warm (Cb) subtropical climates. The HMP/LMP ratios range from 3.15 to 9.89 and fall below the humid/monsoonal threshold, indicating wet climates (Cf) (Table 7). However, at site #05/1, thin section analysis (TH05/1) reveals a monsoonal influence characterized by humid/ dry alteration (Fig. 4D), while palynological analysis (BTP05/1) yields an HMP/LMP ratio of 7.63 (Table 7). Consequently, an HMP/LMP value of 7 may be considered a threshold for monsoonal influence; thus, the following samples may exhibit slight monsoonal influence: BTP05/1, 2, 4, 5; BTP06/2, three and BTP08/1. Based on previous analyses, the samples within the temperate climate group C can be categorized as follows: hot and humid subtropical (Cfa) with slightly monsoonal influence for samples BTP-05/2, BTP-08/1; warm subtropical (Cfb) for samples BTP05/3, BTP06/4, BTP10/1 and BTP19/1; warm subtropical (Cfb) with slightly monsoonal influence for samples BTP05/1, BTP06/2; and undecided between Cfa or Cfb climate for BTP05/4 and 5, BTP06/1 and 3, BTP07/1, BTP13/3, BTP21/2 and BTP23/2.

The sample BTP-24/1 in the Red River Trough, as previously mentioned, may belong to either the temperate group (Cfa/Cfb) or tropical group (A). In the case of group A, the LMP of 19-94 mm suggests the following types: tropical rainforest (Af) if LMP ≥ 60 mm; tropical monsoon (Am) if 43 mm ≤ LMP < 60 mm; and dry savanna in winter (Aw) if LMP < 43 mm due to high WMP.

Table 7. HPM/LPM ratios in analyzed samples

Sample	HPM/LPM	Sample	HPM/LPM
Na Duong basin		**Red River trough**	
BTP-05/1	7.63	BTP-13/3	5.14
BTP-05/2	9.89	BTP-19/1	5.14
BTP-05/3	3.15	BTP-21/2	4.83
BTP-05/4	8.18	BTP-23/2	3.73
BTP-05/5	8.47	BTP-24/1	3.61
BTP-06/1	4.92	Average: 6.16 Min: 3.15 Max: 9.89 Humid/ monsoonal threshold: 10	
BTP-06/2	7.29		
BTP-06/3	7.29		
BTP-06/4	6.27		
BTP-07/1	5.18		
BTP-08/1	8.13		
BTP-10/1	5.86		

5.4. General Oligocene paleoclimate in Northern Vietnam

As determined by ^{18}O isotope analyses, Cenozoic global temperatures underwent significant fluctuations, peaking around ca. 50 Ma during the Eocene. This period was followed by a decreasing trend, particularly from the Oligocene onward, characterized by notable climatic events such as the Oi-1 glaciation during Eocene-Oligocene transition and a high-temperature phase known as Mid-Miocene Climatic Optimum (Zachos et al., 2001; Hansen et al., 2013). Climate change in East Asia was influenced by several factors, including the collision between the Indian and Eurasian plates, the uplift of the Himalayas - Tibetan plateau, and the evolution of the monsoon system (Zhisheng et al., 2001; Yao et al., 2011; Quan et al., 2012). During the Eocene, southern China was dominated by a subtropical or tropical climate (Quan et al., 2012), which evolved into a humid subtropical climate in the Oligocene (Li et al., 2018). By the Miocene, the region exhibited notable seasonality and spatial variations in temperature and precipitation (Yao et al., 2011). In Thailand, the warm temperate climate in the Oligocene to Early Miocene transitioned to a tropical climate in the Middle Miocene, possibly extending to the end of the Early Miocene (Songtham et al., 2003). The Oligocene climate in northern Vietnam, as synthesized from thin-section, XRD, and palynological analyses, was primarily characterized by a warm subtropical type (Cfb), occasionally exhibiting hot and humid (Cfa) or cold and dry periods, with slight influences from the monsoon (Table 8). This characterization is consistent with the broader climatic context of the South China-North Thailand-North Vietnam region. Monsoons currently dominate this region with a monsoonal tropical climate (Am) in northern Thailand and hot-or-warm summer subtropical climates (Cwa, Cfa) in north Vietnam and southern China (Fig. 11). So, compared to the present, the Oligocene climates are colder and less influenced by monsoons.

In the Hoanh Bo basin, based on the dominance of reddish and red-brown beds of ferric oxide-rich cemented sandstones, the presence of thin ironstone caps within fine-grained grey rocks, the intercalation of lacustrine sediments between shale and thin layers of reddish wacke, presence of very large siderite concretion (up to 30 cm in size) and the thick layers of gypsum, Tha et al. (2017) indicated a semi-arid hot climate with a high thermal background intercalated with short humid cycles for Dong Ho Formation. However, Vuong and Hoai (2018) proposed that the sediments of the Dong Ho formation were derived from strongly weathered bedrock, as indicated by high weathering

indices such as Chemical Index of Alteration (CIA: 88.32-93.17), Chemical Index of Weathering (CIW: 94.50-99.32), Plagioclase Index of Alteration (PIA: 94.39-99.35) and Chemical Proxy of Alteration (CPA: 97.75-99.75), reflecting a humid climate with a MAP, determined by CIW, of 1533±181 mm/y during the sedimentation. Wysoka et al. (2022) suggested a shift from a humid tropical to a humid subtropical climate in the sediments of the Hoanh Bo Trough, with high CIW (95-99) and PIA (94-99) values similar to those of Vuong and Hoai (2018), indicating a high degree of chemical weathering. The CIA values ranged from moderate (for four samples in the Hoanh Bo area) to strong weathering conditions (for two samples in the Dong Ho area). For all samples taken from the Hoanh Bo area in this study, thin-section analyses revealed unweathered conditions with (semi)arid characteristics for samples TH02/1 and TH04/1, while sample TH03/4 exhibited moderate weathering under subhumid or humid conditions (Fig. 8). XRF analyses of samples R02/2 and R03/4 indicated hot and humid conditions, characterized by a predominance of kaolinite and high ratios of kaolinite/illite or kaolinite/(illite + chlorite) (Table 6). These analyses suggest hot-humid climates (Cfa) and cold-dry climates (Cfb) for samples in the Hoanh Bo area (Table 8).

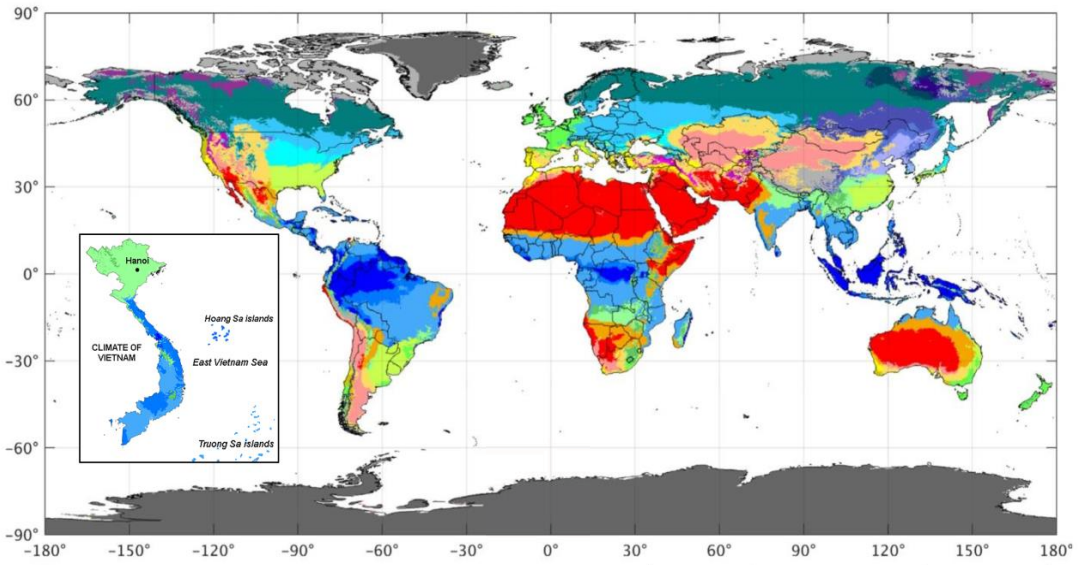

1st letter	2nd letter	3rd letter
A (Tropical)	f (Rainforest) m (Monsoon) w (Savanna, dry winter) s (Savanna, dry summer)	
B (Dry)	W (Arid Desert) S (Semi-Arid or steppe)	h (Hot) k (Cold)
C (Temperate)	w (Dry winter) f (No dry season) s (Dry summer)	a (Hot summer) b (Warm summer) c (Cold summer)
D (Continental)	w (Dry winter) f (No dry season) s (Dry summer)	a (Hot summer) b (Warm summer) c (Cold summer) d (Very cold winter)
E (Polar)	T (Tundra) F (Ice cap)	

Figure 11. Köppen-Geiger climate present-day map (1980-2016) Beck et al., 2018

Table 8. Oligocene climate in Northern Vietnam

Depression	Site	Thin section	XRD	Palynology	General Climate
Hoanh No	#02/1	Iw=0; unweathered; (semi)arid climate or mountains,			Cfb?
	#02/2		Hot, humid		Cfa
	#03/4	Iw=2; moderately weathered; the subhumid climate in plains or humid climate in hills	Hot. humid		Cfa
	#04/1	Iw =0; unweathered; (semi) arid climate or mountains			Cfb?
Na Duong	#05/1		Seasonal (dry/humid)	Cfb	Cfb, monsoon influence
	#05/2			Cfa ,	Cfa, monsoon influence
	#05/3			Cfb	Cfb
	#05/4	Iw=1; slightly weathered; subhumid climate in hills		Cfa/Cfb	Cfb, monsoon influence
	#05/5			Cfa/ Cfb	Cfb, monsoon influence
	#06/1			Cfa/Cfb	Cfa/Cfb
	#06/2			Cfb	Cfb, monsoon influence
	#06/3			Cfa/Cfb	Cfa/Cfb, monsoon influence
	#06/4			Cfb	Cfb
	#07/1			Cfa/Cfb	Cfa/Cfb
	#07/2		Slightly hot and humid		Cfb
	#07/3		Cold, dry		Cold, dry
	#08/1			Cfa	Cfa
	#09/1	Iw=2; moderately weathered; subhumid climate in plains or humid climate in hills			Cfb
	#10/1			Cfb	Cfb
Red River Trough	#13/3			Cfa, Cfb	Cfa, Cfb
	#15/1	Seasonal (dry/humid change)			Cfb, monsoon influence
	#19/1		Cold, dry	Cfb	Cfb
	#19/2		Cold, dry		Cfb
	#21/2			Cfa, Cfb	Cfa, Cfb
	#23/2		Cold , dry	Cfa, Cfb	Cfb
	#24/1		Cold, dry		Cfb
	#24/2	Iw =0; unweathered; (semi)arid climate or mountains,		Af, Am, Aw, Cfa, Cfb	Cfb

In the Red River Trough, the Oligocene warm subtropical climate (Cfb) expressed more continental, dry, and cold features with a MAT ranging from 9.3 to 22.2°C and a MAP of 1122 to 1857 mm for the majority of analyzed samples. Overall, the Oligocene climate in this region was colder and drier than the present. The climate suggested by Hung et al. (2022), with a MAT of 15.4 to 22.6°C and a MAP of 1302.3 to 2164 mm, is based solely on the presence of the species Mucuna birdwoodiana in sample taken from Co Phuc Formation and its current NLR distribution in China. This climatic estimate reflects only a specific moment rather than the entire Oligocene. However, this suggestion is consistent with the region's previously mentioned general climate conditions.

In the Na Duong basin, the Oligocene climate is characterized primarily as warm subtropical (Cfb), occasionally alternating with hot and humid subtropical periods (Cfa), likely influenced by monsoons. Most palynologically analyzed samples indicate a MAT ranging

from 9.3 to 21.7°C and a MAP between 1122 and 1724 mm. Notably, all analyzed samples from the Na Duong basin were collected in stratigraphic order, allowing for the assessment of temporal variations in paleoclimate (Fig. 2). Analyses of pollen and spores reveal that the average of MAT and MAP in most samples are lower than the current MAT and higher than the current MAP (Fig. 12). Although these average values do not precisely reflect the paleoclimatic parameters, they can still be used to evaluate climate variability. Except for the segment between BTP08/1 and BTP07/1, the cross-section indicates climate changes that show a trend of simultaneous increases or decreases in temperature and precipitation, resulting in either a hotter-wetter or colder-drier climate. Notably, the segment from BTP05/5 to BTP05/1, sampled with ca. 1 m resolution across different lithological layers at the same site, reveals colder and drier climates in BTP05/5 and BTP05/3, contrasted with hotter and wetter climates in BTP05/4, BPT05/2, and BPT05/1.

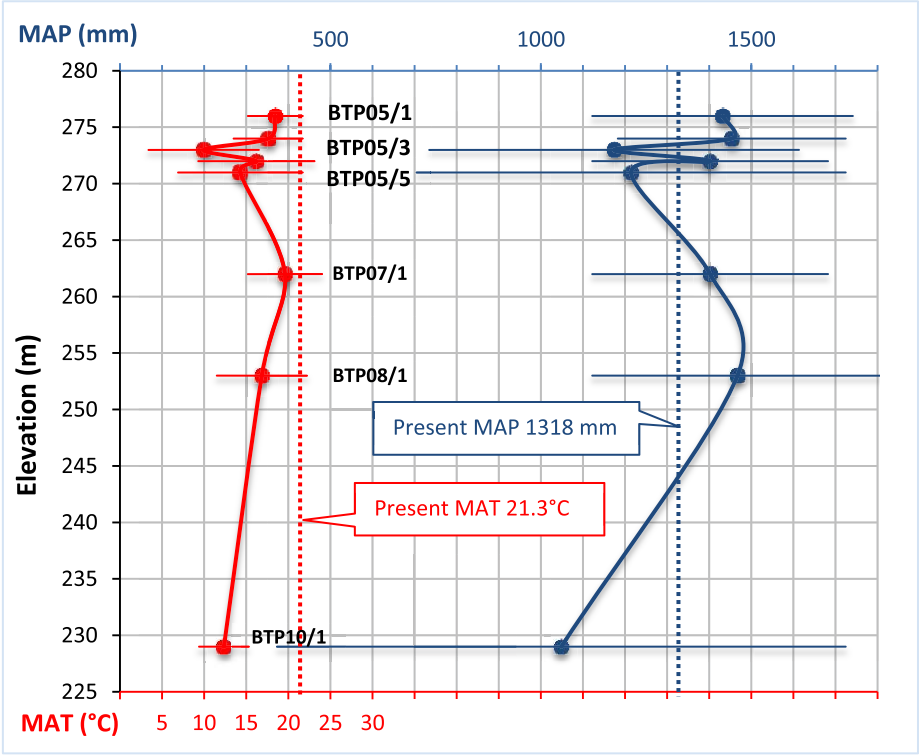

Figure 12. MAT and MAP resulted from palynological analyses in Na Duong basin

Similarly, climate variation in the Na Duong basin, resulting from variations in percentages of quartz and feldspar, the total clay minerals, and the ratios of kaolinite/illite and (kaolinite+smectite)/(illite + chlorite) (Fig. 13), shows a tendency to increase temperature and humidity from R09/1 to R07/2, with a maximum value at R07/2 characterized by high ratios of kaolinite/illite and (kaolinite+smectite/(illite + chlorite). Notably, the percentages of quartz and feldspar and the total clay minerals in R07/2 are relatively low due to a significant percentage of siderite (34%) (Table 4). In the subsequent period, R07/1-R05/3, the climate becomes drier and colder, as evidenced by

decreased values in the percentage of clay minerals, the ratios of kaolinite/illite, and (kaolinite + smectite)/(illite + chlorite). Following this period, the climate reverses, exhibiting a warmer and wetter trend.

For the Na Duong basin, based on the presence of Dipterocaparaceae, a group of crocodile fossils, and sediment characteristics lacking indicators of well-oxygenated paleosols or pedogenic carbonate accumulation, Böhme et al. (2013) suggested a tropical to warm subtropical climate during the formation of the Na Duong basin, with lower limit MAT >14.2°C and CMT >5.5°C, indicating per humid conditions without a dry season. Additionally, the spore-pollen analysis conducted by Wysocka et al. (2020) suggests a warm temperate to subtropical paleoclimate for the Na Duong basin. Thus, the climates defined by Köppen-Geiger as warm subtropical (Cfb), occasionally alternating with hot and humid subtropical periods (Cfa) and likely monsoonal influence, are relatively consistent with the findings of Böhme et al. (2013) and Wysocka et al. (2020) as inferred from thin section, XRD and palynological analyses.

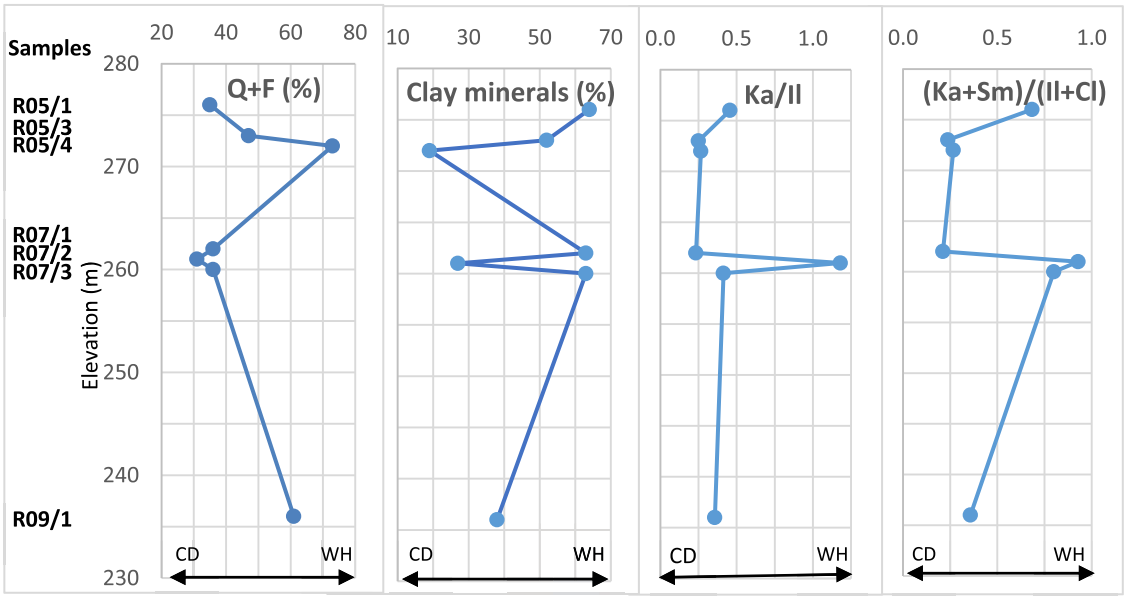

Figure 13. Content of quartz+feldspar (%), clay minerals (%) and clay mineral ratios in Na Duong basin (Q- quartz, F-feldspar, Ka-Kaolinite, Sm-Smectite, Il-Illite, Cl-chlorite, CD-cold dry, WH-warm humid)

6. Conclusions

The formation of Dong Ho (Hoanh Bo basin), Na Duong (Na Duong basin), and Co Phuc (Red River Trough) in northern Vietnam is primarily composed of conglomerate, gritstone, sandstone, siltstone, claystone, and coal shale, all deposited in continental environments. Based on the palynomorph assemblages, these formations can be dated to Oligocene. During this period, the paleoclimate was characterized mainly by a warm subtropical type (Cfb), occasionally experiencing hot and humid (Cfa) or cold and dry periods, with slight influences from monsoons.

In the Hoanh Bo basin, analyses indicate the presence of both hot-humid and cold-dry climates. In the Red River Trough, the Oligocene climate was colder and drier than the present. This climate is characterized as a warm subtropical climate (Cfb), exhibiting

more continental, dry, and cold features, with a MAT ranging from 9.3 to 22.2°C and a MAP between 1122 mm and 1857 mm.

In the Na Duong basin, the Oligocene climate is characterized primarily by a warm subtropical (Cfb), occasionally alternating with hot and humid subtropical periods (Cfa), likely influenced by monsoons. Most palynologically analyzed samples indicate a MAT ranging from 9.3 to 21.7°C and a MAP between 1122 and 1724 mm. Temporal variations in temperature and precipitation exhibit similar patterns, suggesting an alternation between dry-cold or humid-hot phases.

Acknowledgments

This article is supported by the project coded CSCL11.03/22-23.

References

Adatte T., Keller G., Stinnesbeck W., 2002. Late Cretaceous to early Paleocene climate and sea-level fluctuations: the Tunisian record. Palaeogeogr. Palaeoclimatol. Palaeoecol., 178, 165–196.

Bat D., Ngoc N., Hoi N.V., Hieu D.V., Hong N.T., Quang C.D., 2008. Paleontological stratigraphy: 30-year development of Vietnam's petroleum geology. Proceedings of Science and Technology conference "Vietnam Oil and Gas Institute: 30 years of development and integration". Science and Technology, Hanoi, 76–85 (in Vietnamese).

Beck H.E., Zimmermann N.E., McVicar T.R., Vergopolan N., Berg A., Wood E.F., 2018. Data Descriptor: Present and future Köppen-Geiger climate classification maps at 1 km resolution. Scientific Data, 5, 180214. Doi: 10.1038/sdata.2018.214

Böhme M., Aiglstorfer M., Antoine P.O., Appel E., Havlik P., Métais G., Phuc L.T., Schneider S., Setzer F., Tappert R., Tran D.N. , Uhl D., Prieto J., 2013. Na Duong (northern Vietnam) - an exceptional window into Eocene ecosystems from Southeast Asia. Zitteliana Reihe A, 53, 121–167.

Chamley H., 1989. Clay Sedimentology. Springer-Verlag, New York, NY, USA.

Chen T., Wang H., Zhang Z.Q., Wang H.J., 2003. Clay minerals as indicators of paleoclimate. Acta Petrol. Mineral, 22, 416–420.

Chung S.L., Lee T.Y., Lo C.H., Wang P.L., Chen C.Y., Yem N.T., Hoa T.T., Genyao W., 1997: Intraplate extension prior to continental extrusion along the Ailao Shan-Red River shear zone. Geol., 25, 311–314. Doi: 10.1130/0091-7613(1997)025<0311: IEPTC E>2.3.CO; 2.

Ducloux J., Meunier A., Velde B., 1976. Smectite, chlorite and a regular interlayered chlorite-vermiculite in soils developed on a small serpentinite body, Massif Central, France. Clay Min., 11, 121–135.

Duong N.T., Linh N.M., 2011. Characteristics of pollen and spore in sediment of the Hanoi area in relation to climate and vegetation change in Holocene. Vietnam J. Earth Sci., 33(3), 297–305 (in Vietnamese).

Ehrmann W., 1988. Implications of late Eocene to early Miocene clay mineral assemblages in McMurdo Sound (Ross Sea, Antarctica) on paleoclimate and ice dynamics. Palaeogeogr. Palaeoclimatol. Palaeoecol., 139, 213–231.

Folk R. L., 1968. Petrology of Sedimentary Rocks. Austin, Texas, Hemphill, 182p.

Geiger R., 1954. "Klassifikation der Klimate nach W. Köppen" [Classification of climates after W. Köppen]. Landolt-Nörnstein - Zahlenwerte und Funktionen aus Physik, Chemie, Astronomie, Geophysik und Technik, alte Serie. Berlin. Springer, 3, 603–607.

Gingele F.X., Deckker P.D., Hillenbrand C.D., 2001. Late Quaternary fluctuations of the Leeuwin Current and palaeoclimates on the adjacent land masses: Clay mineral evidence. J. Geol. Soc. Aust, 48, 867–874.

Grimm G.W, Bouchal J.M., Denk T., Potts A., 2016. Fables and foibles: A critical analysis of the Palaeoflora database and the Coexistence Approach for palaeoclimate reconstruction. Rev. Palaeobot. Palynol., 233, 216–235. http://doi.org/10.1016/j.revpalbo.2016.07.001.

Hansen J., Sato M., Russell G. and Kharecha P., 2013. Climate sensitivity, sea level and atmospheric carbon dioxide. Phil. Trans. R. Soc.

A., 371, 20120294. http://dx.doi.org/10.1098/rsta.2012.0294.

Huang J., Spicer R.A., Li S.-F., Liu J., Do T.V., Nguyen H.N., Zhou Z.-K., Su T., 2022. Long-term floristic and climatic stability of northern Indochina: Evidence from the Oligocene Ha Long flora, Vietnam. Palaeogeogr. Palaeoclimatol. Palaeoecol., 593, 110930. https://doi.org/10.1016/j.palaeo.2022.110930.

Hung N.N., Huang J., Do T.V., Jia L.N., Hoa M.T.N., Hung D.D., Li S.F., Zhou Z.K, Su T., 2022. First pod record of Mucuna (Papilionoideae, Fabaceae) from the Late Miocene of the Yen Bai Basin, northern Vietnam. Review of Palaeobotany and Palynology, 298, 104592.

Huong N.V., Unkel I., Duong N.T., Thai N.D., Quoc D.T., Tung D.X., Hong N.T., Thanh D.X., Nguyet N.T.A., Quan N.H., Hoan D.T., Trang N.T.H., Nhung P.L.T., Anh L.N., Ha V.V., Ojala A.E.K., Schimmelmann A., Sauer P., 2023. Paleoenvironment potential of lacustrine sediments in the Central Highland of Vietnam: a review on the state research. Vietnam J. Earth Sci., 45(2), 164–182. https://doi.org/10.15625/2615-9783/18281.

Huyen N.X., Pha P.D., Hung N.Q., 2004. Historical development of Paleogene - Neogene sedimentary formations in relation to the Red River fault. In the Red River Fault Zone. Geodynamic characteristics, mineralogy and natural disasters. Science and Technics Publishing House, Hanoi, 413–462 (in Vietnamese).

Jain M., Tandon S.K., 2003. Quaternary alluvial stratigraphy and palaeoclimatic reconstruction at the Thar margin. Curr. Sci., 84, 1048–1055.

Jimenez-Espinosa R., Jimenez-Millan J. , 2003. Calcrete development in mediterranean colluvial carbonate systems from SE Spain. J. Arid Environ., 53, 479–489.

Jiménez-Moreno G., Fauquette S., Suc J.P, 2010. Miocene to Pliocene vegetation reconstruction and climate estimates in the Iberian Peninsula from pollen data. Review of Palaeobotany and Palynology, 162, 403–415.

Keller W.D., 1970. Environmental aspects of clay minerals. J. Sediment. Res., 40, 788–859.

Köppen W., 1884. Translated by Volken, E.; Brönnimann, S. "Die Wärmezonen der Erde, nach der Dauer der heissen, gemässigten und kalten Zeit und nach der Wirkung der Wärme auf die organische Welt betrachtet" [The thermal zones of the earth according to the duration of hot, moderate and cold periods and to the impact of heat on the organic world)]. Meteorologische Zeitschrift (published 2011), 20(3), 351–360. Bibcode: 2011MetZe..20..351K. doi:10.1127/0941-2948/2011/105. S2CID 209855204.

Ky H.N. (editor), Bac D.D., Du D.C, Thang N.Q., Luong N.C, Kha N.D., Nhat N.T., My N.Q., Thinh N., Thang T.H., Khuyen T.X., 2000. Geological and mineral resources map of Vietnam on 1:200,000. Lang Son Sheet. Department of Geology and Minerals of Vietnam.

Ky H.N. (editor), Quan D.T., Hoa De H.T., Kham L.D., Minh N.N., Chu N.T., 1999. Geological and mineral resources map of Vietnam on 1:200,000. Hai Phong Sheet. Department of Geology and Minerals of Vietnam.

Lacassin R., Leloup P.H., Tapponnier P., 1993. Bounds on strain in large Tertiary shear zones of SE Asia from boudinage restoration. J. Struc. Geol., 15, 677–692

Lan L.T.P., Ellwood B.B., Su N.K., Wang W.H., Lam D.D., Dung N.T., Mai N.T., 2023. High-resolution record of paleoclimate during the late Quarternary, recovered from Con Moong cave-North Vietnam. Vietnam J. Earth Sci., 45(3), 374–387. https://doi.org/10.15625/2615-9783/18576.

Lee T.Y., Lawver L.A., 1995: Cenozoic plate reconstruction of Southeast Asia. Tectonophysics, 251, 85–138. Doi: 10.1016/0040-1951(95)00023-2.

Leloup P.H., Lacassin R., Tapponnier P., Schärer U., Dalai Z., Xiaohan L., Liangshang Z., Shaocheng J. and Trinh P.T., 1995. The Ailao Shan-Red River shear zone (Yunnan China), Tertiary transform boundary of Indochina. Tectonophysics, 25, 3–84.

Li P., Zhang C., Guo Z., Deng C., Ji X., Jablonski N.G., Wu H., Zhu R., 2019. Clay mineral assemblages in the Zhaotong Basin of southwestern China: Implications for the late Miocene and Pliocene evolution of the South Asian monsoon. Palaeogeogr. Palaeoclimatol. Palaeoecol., 516, 90–100.

Li S., Xing Y., Valdes P.J. , Huang Y., Su T. , Farnsworth A., Lunt D.J., Tang H. , Kennedy A.T., Zhou Z., 2018. Oligocene climate signals and forcings in Eurasia revealed by plant macrofossil and modeling results. Gondwana Research, 61, 115–127.

Long H., Wang C.H., Liu Y.P., Ma H.Z., 2007. Application of clay minerals in paleoenviroment research. J. Salt Lake Res., 15, 21–25.

Long H.V., Clift P.D., Schwab A.M., Huuse M., Anh N.D., Sun Z., 2010. Large-scale erosional response of SE Asia to monsoon evolution reconstructed from sedimentary records of the Song Hong-Yinggehai and Qiongdongnan Basins, South China Sea (East Sea). In: Clift, PD, Tada, R. & Zheng, H. (eds) Monsoon Evolution and Tectonics-Climate Linkage in Asia. Geological Society, London, Special Publications, 342, 219–244. Doi: 10.1144/SP342.13 0305-8719/10.

Long H.V., Wu, F.Y., Clift, P.D., Wysocka, A., Swierczewska, A., 2009. Evaluating the evolution of the Red River system based on in situ U-PN dating and Hf isotope analysis of zircons. Geochem. Geophys. Geosyst. 10, Q11008.

Longiaru S., 1987. Visual comparators for estimating the degree of sorting from plane and thin section. J. Sed. Res., 57(4), 791–794. https://doi.org/10.1306/212F8C60-2N24-11D7-8648000102C1865D.

Luong N.C. (editor), Nong C.Q., Do D.V., Tiep D.V., Nguyen L.D., Thang N.Q., Dung N.H., Thanh N.Q., Duong T.C., Hung V.V., 1999. Geological and mineral resources map of Vietnam on 1:200,000. Ha Long Sheet (Hon Gai). Department of Geology and Minerals of Vietnam.

Meunier A., 1980. Les mécanismes de l'altération des granites et le rôle des microsystèmes. Etude des arénas du massif granitique de Parthenay (Deux-Sèvres). Mém. Soc. Geol. Fr., 140, 1–80.

Mosbrugger V., Utescher T., 1997. The coexistence approach a method for quantitative reconstructions of Tertiary terrestrial palaeoclimate data using plant fossils. Palaeogeogr. Palaeoclimatol. Palaeoecol., 134, 61–86.

Naidu A. S., Han M. W., Mowatt T. C., Wajda W., 1995. Clay minerals as indicators of sources of terrigenous sediments, their transportation and deposition: Bering Basin, Russian-Alaskan Arctic. Marine Geology, 127, 87–104.

Nghi T., Than T.H., Lan N.T., Thanh D.X., Minh D.Q, Nhan T.T.T., Vu P.N.H., 2004. Developing stages of Cenozoic sedimentary of the Red River basin in relation to Geodynamic activities. Vietnam. J. Earth Sci., 26(3), 193–201 (in Vietnamese).

Picard M.D., 1971. Classification of fine-grained sedimentary rocks. J. Sed. Res., 41(1), 179–195. doi: https://doi.org/10.1306/74D7221N-2N21-11D7-8648000102C1865D.

Pross J., Bruch A.A., Mosbrugger V., Zlatko K.Z., 2001. Paleogene pollen and spores as a tool for quantitative paleoclimate reconstructions: the Rupelian (Oligocene) of Central Europe. Print: Goodman DK and Clarke RT (eds), Proceeding of the IX International Palynological Congress, Houston, Texas, USA, 1996; America Association of Stratigraphic Palynologists Foundation, 299–310.

QCVN-02:2022/NXD, 2022. National technical regulation on data of natural conditions used in construction. Vietnam National Technical Regulation on Natural Physical and Climatic Data for Construction, Hanoi.

Quan C., Liu Y.S., Utescher T., 2012. Eocene monsoon prevalence over China: A paleobotanical perspective. Palaeogeogr. Palaeoclimatol. Palaeocol, 365–366, 302–311.

Quang N.M., Ha V.V, Min N.T., Dao N.T., Cuc N.T.T., Tuan D.M., Tung D.X., Man T.T., Thao N.T., 2023. Holocene sedimentary facies in the incised valley of Ma River Delta, Vietnam. Vietnam J. Earth Sci., 45(4), 497–516. https://doi.org/10.15625/2615-9783/18923.

Song Z., 1996. Early Tertiary normapolles and related palynomorphs of China. Taiwania, 41(1), 53–57.

Songtham W., Ratanasthien N., Mildenhall DC, Singharajwarapana S. and Kandharosaa W., 2003. Oligocene-Miocene climatic changes in Northern Thailand resulting from extrusion tectonics of Southeast Asian landmass. ScienceAsia, 29, 221–233.

Steinmann Institute, Bonn University. Paleobotanical climate data. http://www.palaeoflora.de.

Sun G., Zhang S., Wang Y., Li Y., Guo H. Bo, S., 2022. Eocene sedimentary-diagenetic environment analysis of the Pingtai Area of the Qaidam Basin. Appl. Sci, 12, 6850. https://doi.org/ 10.3390/app12146850.

Suttner L.J., Basu A., Mack G.H., 1981. Climate and the origin of quartz arenite. J. Sed. Petrol., 51, 1235–1244.

Tapponnier P., Peltzer G., Armijo R., 1986. On the mechanics of the collision between India and Asia. Geol. Soc. London. Spec. Publ., 19, 113–157. Doi: 10.1144/ GSL.SP.1986.019.01.07.

Tha H.V., Iqbal S., Czarnieca U., Wysocka A., Pha P.D., Cuong N.Q., Ha V.V., Tuan D.M., 2021. Geochemistry and mineralogy of the Truc Thon Clay, Hai Duong Province, North Vietnam: implication for paleoclimatic and provenance analysis. Vietnam J. Earth Sci., 43(4), 524–545. https://doi.org/10.15625/2615-9783/16572.

Tha H.V., Wysoka A., Cuong N.Q., Pha P.D., Ziółkowski P., 2017 Sedimentary petrology characteristics and their implications for provenance of Hoanh Bo basin Neogene system in Quang Ninh province, northeastern Vietnam. Geology, Geophysics & Environment, 43(1), 69–87.

Tha H.V., Wysoka A., Pha P.D., Cuong N.Q., Ziółkowski P., 2015. Lithofacies and depositional environments of the Paleogene/Neogene sediments in the Hoanh Bo Basin (Quang Ninh province, NE Vietnam). Geology, Geophysics & Environment, 41(4), 353–369.

Thamban M., Rao V.P., 2005. Clay minerals as palaeomonsoon proxies: evaluation and relevance to the late Quaternary record from SE Arabian Sea. In: Rajan, S., Pandey, P.C. (Eds.), Antarctic Geoscience: Ocean-atmosphere Interaction and Paleoclimatology. National Centre for Antarctic & Ocean Research, Goa, India, 198–215.

Thanh T.D., Khuc V. (eds), Huyen D.T., Truong D.N., Bat D., Dy N.D., Hung N.H., Thong P.H., Ngan P.K., Phuong T.H, Dan T.H., Thang T.T., Tri T.V., Long T.V., 2005. Stratigraphic units of Vietnam. Hanoi National University Publishing House. Hanoi, 526p.

Thiry M., 2000. Palaeoclimatic interpretation of clay minerals in marine deposits: an outlook from the continental origin. Earth-Sci. Rev., 49, 201–221.

Thuan D.V., Dao N.T., Tan M.T., Luong L.D., Ha T.T.T., Tao N.V., 2019. Biostratigraphic features of Late Miocene coal-bearing sediments in the Southeast of the Red River Delta. VNU J. Sci.: Earth and Environmental Sci., 35(2), 114–129 (in Vietnamese).

Trinh P.T., Liem N.V., Huong N.V., Vinh H.Q., Thom N.V., Thao N.T., Tan M.T., Hoang N., 2012. Late Quaternary tectonics and seismotectonics along the Red River fault zone, North Vietnam. Earth-Sci. Rev., 114, 224–235.

Trung P.Q., Bat D., An N.Q., Khoi D.V, Hieu D.V., 1999. The new documentation of spore and pollen fossil in the Dong Ho Formation. Petrovietnam J., 3, 2–8 (in Vietnamese).

Trung P.Q., Nguyen Q.A., Do B.., Nguyen V.H., Luu K.T., Chu D.Q., Le T.T.H., Bui V.T., Nguyen T.L,. Duong, H.S., 1998. Palynology assemblages in Paleogene sediments in northern Song Hong basin and the adjacent areas, their relationship with the sedimentary environment. basic research results from 1996 to 1998. Vietnam Petroleum Institute, Ha Noi (in Vietnamese).

Trung P.Q., Quynh P.H., Bat D., An N.Q., Khoi D.V., Hieu D.V., Ngoc, N., 2000. New palynological investigation in the Na Duong mine. Petrovietnam J., 7, 18–27 (in Vietnamese).

Utescher T., Bruch A.A, Erdei N., François L.M., Ivanov D., Jacques F.M.N, Kern A.K , Liu Y.S.(C.), Mosbrugger V., Spicer R.A., 2014. The Coexistence Approach Theoretical background and practical considerations of using plant fossils for climate quantification. Palaeogeography, Palaeoclimatology, Palaeoecology, 410, 58–73. Doi: 10.1016/j.palaeo.2014.05.031.

Vanderaveroet P., 2000. Miocene to Pleistocene clay mineral sedimentation on the New Jersey shelf. Oceanol. Acta, 23, 25–36.

Velde B., 1992. Introduction to clay minerals: Chemistry, origins, use and environmental significance. Chapman & Hall, London, 113–163.

Vinh N. (editor), Gulaiev I.S., Thuy D.K., Luong N.C., Thi P.T., 2005. Geological and mineral resources map of Vietnam 1:200,000. Yen Bai Sheet. Department of Geology and Minerals of Vietnam.

Vuong N.V. and Hoai L.T.T., 2018. Geochemistry of major and trace elements of sediments of Dong Ho, Quang Ninh formations and their significance in determining ancient environmental conditions. VNU J. Sci.: Earth and Environmental Sci., 34(2), 110–120.

Weltje G.J., 1994. Provenance and dispersal of sand-sized sediments: Reconstruction of dispersal patterns and sources of techniques. PhD dissertation, Utrecht University. Geologica Ultraiectina, 208p.

Weltje G.J., Meijer X.D. and De Noer P.L., 1998, Stratigraphic inversion of siliciclastic basin fills: a note on the distinction between supply signals resulting from tectonic and climatic forcing. In: Hovius, N., Leeder, M. (Eds.), Thematic Set on Sediment Supply to Basins. Basin Research, 10, 129–153.

Wysocka A. and Swierczewska A., 2010. Lithofacies and depositional environments of Miocene deposits from tectonically-controlled basins (Red River Fault Zone, northern Vietnam). J. Asian Earth Sci., 39, 109–124.

Wysocka A., Pha D.P., Durska E., Czarnieckac U., Thang D.V., Filipek A., Cuong N.Q., Tuan D.M., Huyen N.X., Tha H.V., Staniszewski R., 2020. The Na Duong basin (North Vietnam): A key for understanding Paleogene basin evolution in relation to the left-lateral Cao Nang-Tien Yen Fault. J. Asian Earth Sci., 195, 104350. https://doi.org/10.1016/j.jseaes.2020.104350.

Wysocka A., Tha H.V., Czarniecka U., Durska E., Filipek A., Pha P.D., Cuong N.Q., Zaszewski D., Tuan D.M., Thanh N.T., Naranowski A., 2022. The Hoanh Bo Trough - a landward keyhole to the syn-rift Late Eocene-Early Oligocene terrestrial succession of the northern Song Hong basin (onshore north-east Vietnam). Geological Journal, 1–26. Doi: 10.1002/gj.4539.

Yao Y.F., Bruch A.A., Mosbrugger V., Li C.S., 2011. Quantitative reconstruction of Miocene climate patterns and evolution in Southern China based on plant fossils. Palaeogeogr. Palaeoclimatol. Palaeoecol., 304, 291–307.

Zachos J., Pagani M., Sloan L., Thomas E., Billups K. 2001. Trends, rhythms, and aberrations in global climate 65 Ma to present. Science, 292, 686–693. Doi: 10.1126/science.1059412.

Zhisheng A., Khutzbach J.E., Prell W.L., Porter S.S., 2001. Evolution of Asian monsoons and phased uplift of the Himalaya Tibetan plateau since Late Miocene times. Nature, 411, 62–66.

Zuchiewicz W., Cuong N.Q., Zasadni J., Yem N.T., 2013. Late Cenozoic tectonics of the Red River Fault Zone, Vietnam, in the light of geomorphic studies. Journal of Geodynamics, 69, 11–30. Doi: 10.1016/j.jog.2011.10.008.